Periodicity in Extreme Weather in the 'Maritime Region' of Eastern North America

Carling Ruth Walsh (carling.walsh@carleton.ca)
Carleton University
R. Timothy Patterson
Carleton University

Research Article

Keywords: extreme weather, solar AMO NAO AO ENSO QBO teleconnections, climate change, eastern North America, Maritimes, time series analysis

Posted Date: March 11th, 2021

DOI: https://doi.org/10.21203/rs.3.rs-280154/v1

Abstract

Spectral and wavelet analysis were used to identify trends and cycles in extreme temperature and precipitation events based on historical data (~100-150 years) from six climate stations within the “Maritime Region” of eastern North America. Many statistically significant climate cycles were identified using both spectral and Morlet wavelet analyses at each of these locations for both extreme high and low temperature and precipitation (rain, snow) data, with periodicities typically ranging from ~ 2–30 years. To assess potential drivers of these cyclical extreme weather events, the records of these events were compared, using cross wavelet analysis, to the climate indices of several teleconnections, including the 11-year Schwabe solar cycle, Atlantic Multidecadal Oscillation, North Atlantic Oscillation, Arctic Oscillation, El Niño Southern Oscillation and the Quasi–Biennial Oscillation. It was found that the 11-year solar cycle had the strongest influence over extreme temperature and precipitation in this region, whereas the remaining oscillations, with the exception the Quasi–Biennial Oscillation, exhibited complex interactions with one another, characterized a variety of both positive and negative modulating effects. The Quasi–Biennial Oscillation was found to drive high–frequency oscillations in extreme weather, particularly extreme precipitation. Overall, the findings of this study indicate that extreme weather events in this region have not substantially increased or decreased in number over time, but have been predominantly influenced by several cyclic climate phenomena.

Introduction

Historically, extreme weather events have posed undeniable risk and consequence to both humans and the environment (Parmesan et al. 2000; Greenough et al. 2001; Znachor et al. 2008; Ummenhofer and Meehl 2017; van de Pol et al. 2017; Campbell et al. 2018; Smith and Sheridan 2019) and have been considered among the highest global risk factors in terms of both likelihood and impact (World Economic Forum 2019). Unlike seasonal weather changes, extreme weather events occur within considerably shorter time frames, rendering them nearly impossible to adapt to which, in turn, can be detrimental to human and ecological health (e.g. heat waves associated with increased emergency medical needs (Dolney and Sheridan 2006); storm-induced disturbances distressing phytoplankton communities (Stockwell et al. 2020)).

Changing patterns in the frequency and intensity of extreme weather events driven by anthropogenically driven climate change potentially represents yet another factor to be considered when developing future risk assessment scenarios. Indeed many studies have already reported evidence of increased frequency and intensity in extreme events (e.g. Rahmstorf and Coumou 2011; Gao et al. 2012; Wang et al. 2015), and based on these results computer modeling predicts a concomitant increase in medical and environmental impacts (Wu et al. 2014; Oliver et al. 2019). In contrast, other researchers suggest that natural cyclic climate oscillations within the relatively short historical climate record dataset is a primary influence on the frequency of extreme events (e.g. Knight et al. 2006; Enfield and Cid-Serrano 2010).

With models forecasting an increase in the frequency of extreme weather throughout North America and other mid–latitude regions, (Cai et al. 2014; Cohen et al. 2014; Wang et al. 2015) analysis of regional data subsets of extreme weather events provide an opportunity to specifically assess more localized trends and cycles, and to ascertain whether they are widespread throughout a given region. Furthermore, such analyses provide an opportunity to directly compare instances of extreme weather to various documented cyclic climate phenomena to determine whether cyclical phenomena constitute localized or regional drivers of extreme weather events. Developing such a regional-scale understanding of the contributors to extreme weather is important to society as localized instances of extreme weather can result in flood damage, dangerous road conditions, increased risk of temperature–related health concerns (e.g. heat stroke, frost bite), and may ultimately be related to a myriad of health and safety hazards, as well as a broader ecological impact (Bouwer 2019).

Understanding whether there are trends and cycles in the occurrence of extreme weather events can also provide important information on changes in climate dynamics, an important metric when measuring overall climate change (Linnenluecke et al. 2012; Moazami et al. 2019). Analysis of extreme weather phenomena has also received increased scrutiny within the climate change research community in recent years as new information on the broad impacts of extreme weather has emerged (Ummenhofer and Meehl 2017; Bouwer 2019)

This study examined trends and patterns in daily extreme high and low temperature and precipitation (rain, snow) in eastern North America, specifically a regional subset informally dubbed here as the Maritime Region (MR; see section 4.3 below) and comprising historical weather records from 24 stations in New Brunswick, Nova Scotia, Prince Edward Island, eastern Maine and the Gaspé region of Quebec. Historical records selected for detailed analysis in the MR comprised stations with near-continuous instrumental data records spanning the past 100–150 years. Spectral, Morlet wavelet and cross wavelet time series analysis techniques were then employed to detect trends and patterns within individual records, and to determine whether they correlate with trends and cycles in the records of known drivers of climate in the region (Bonsal and Shabbar 2011; Patterson and Swindles 2015).

Previous Work

Most previous studies that have examined extreme weather phenomena within or near the MR study area have not been carried out to understand the nature of extreme weather itself, but instead have principally either assessed the impact of these events on the environment factors (Payette et al. 1985; Scott et al. 2003; Boland et al. 2004; Andalo et al. 2005; Nye et al. 2009; Ugarte et al. 2010; Lemieux and Scott 2011), or have focused on the influence of extreme weather on human health and safety (Andrey et al. 2003; Dolney and Sheridan 2006; Ziska et al. 2008; Balbus and Malina 2009; Cheng et al. 2012; Wu et al. 2014).

Amongst the few studies that have focused on the incidence of extreme weather phenomena Douglas and Fairbank (2010) for example, examined trends in extreme precipitation in New England, finding that

the trend in extreme precipitation in New England was stationary (near–zero linear slope) from 1893–2005, although some select stations did shown a positive linear trend. In contrast, Frei et al. (2015) identified a pattern of decadal fluctuations in the frequency of extreme precipitation events in the northeastern United States, and an increase in the occurrence of extreme precipitation events during the warm season (June–October) through the twentieth century. Other studies have reported on general trends in extreme weather across other parts of eastern North America outside the MR, presenting evidence of general increases in frequency or intensity of both extreme temperature and extreme precipitation (Bonsal et al. 2001; Zhang et al. 2001; Vincent et al. 2018; Tan and Gan 2017).

Cyclical Drivers Of Regional Climate Change

Drivers of climate oscillations known to impact weather in eastern North America include the Schwabe sunspot cycle (SSC, ~11 years), Atlantic Multidecadal Oscillation (AMO, 50–90 years), El Niño Southern Oscillation (ENSO, 2–10 years), and Quasi–Biennial Oscillation (QBO, 2.1– 2.5 years). The North Atlantic Oscillation (NAO) and Arctic Oscillation (AO) are also known to influence eastern North American weather patterns, though these oscillations do not have well defined periodicities.

3.1 Sunspot Cycle (SSC)

The SSC, which is characterized by the quasi–periodic rise and fall in the number of observed sunspots, cycles approximately every 11 years (9–14 year variability in duration; Lassen and Friis-Christensen 1995; Hathaway 2010, 2015; Jørgensen et al. 2019). Variations in the number of sunspot numbers are related to changes in total solar irradiance and solar variations have been shown to affect temperatures on both long and short timescales. Waple et al. (2002) through proxy record analysis demonstrated both long- and short-term correlations between changes in solar irradiance and global temperature from 1650 – 1850 A.D. A suite of mechanisms control the influence of solar irradiance on the Earth's atmosphere, which can be simplified to two main mechanisms: dynamic changes in the troposphere caused by stratospheric ozone absorption of UV light, and tropospheric heating due to increased solar irradiance (Gray et al. 2010; Rind et al. 2008; Lockwood 2012).

Earlier studies of North American climate patterns have noted the presence of ~11-year cycles in temperature and precipitation that have generally been attributed to the influence of the SSC. For example, Vines (1984) noted the presence of 9.5 and 11 year cycles in rainfall between 1880 – 1960 in the Canadian Maritimes. Similarly, Prokoph et al. (2012) recognized an ~11 year cycle in stream flow records from the St. John River in New Brunswick and the Northeast Margaree River in Nova Scotia. Currie (1988) noted 10 – 11 year cycles in air temperature in New England, as well as throughout the continental USA. Currie and O'Brian (1993) observed 10 – 11 year cycles in New England precipitation records. In fact, the SSC plays a major role in climate variability across the globe. For example, Indian rainfall totals have indicated moderate correlation with the SSC (Ananthakrishnan and Parthasarathy 1984), and both ~11 and ~22 year cycles (22 years being the double sunspot cycle) have been

recognized in Indian, African, and Australian precipitation patterns (e.g. Vines 1977, 1980, 1986; Mazzarella and Palumbo 1992; Currie and Vines 1996; Thresher 2002).

Others have linked the SSC to short term variations in near-surface temperatures in various locations, though many of these studies have focused on latitudinal zones spread across often vast geographical distances (van Loon and Shea 1999 2000; van Loon et al. 2004; Meehl and Arblaster 2009; Meehl et al. 2009; Maliniemi et al. 2014). However, the relationship of the SSC to regional variations in temperature have also been noted in several regional studies, including Romania (Sfîcă et al. 2018), China (Du et al. 2017), and North America (Currie 1993; Mendoza et al. 2001; Mendoza et al. 2006; Nalley et al. 2013).

3.2 Atlantic Multidecadal Oscillation (AMO)

The AMO is an oceanic alternation between warm and cool sea surface temperatures throughout the Atlantic Ocean, characterized by a quasi-periodic ~64-year cycle (~50-90 year variation) with about 30-35 years per phase (Knudsen et al. 2011). There is evidence that the AMO may be derived from an oscillatory component in the strength of North Atlantic thermohaline circulation (Dima and Lohmann 2007), which is characterized by a coherent pattern of warm and cold sea surface phases in the North Atlantic (Schlesinger and Ramankutty 1994). Negative (cold) AMO phases persisted from approximately 1900–1925 and 1965–1995 and positive (warm) phases characterized approximately 1925–1965 and 1995–present (Enfield et al. 2001; Enfield and Cid-Serrano 2010; Knudsen et al. 2011).

AMO positive phases have been associated with several changes in climate, such as decreased precipitation, increased temperature, and droughts in North America (Enfield et al. 2001; Sutton and Hodson 2005, 2007; Nigam et al. 2011). However, in reference to extreme temperatures and precipitation, the AMO has a more prevalent impact on North America by modulating the effects of other climate phenomena (Mo et al. 2009; Zhang et al. 2012; Kang et al. 2014; Park and Li 2019; Zhang et al. 2019). When isolated, significant influence of the AMO by itself on North America often exhibits a coastal-inland gradation (Knight et al. 2006; Patterson and Swindles, 2015). In an analysis of lake ice out records from Maine and New Brunswick, Patterson and Swindles (2015) recognized signals of not only the 32-year AMO phase record, but also ~16-year cycles that they attributed to being secondary subharmonics of the primary AMO multidecadal signal.

3.3 North Atlantic Oscillation (NAO) and Arctic Oscillation (AO)

The NAO is a weather phenomenon caused by fluctuations in atmospheric pressure at sea–level between two pressure centers in the North Atlantic; the Azores High and the Icelandic Low. Variation in this differential pressure influences the strength and directionality of North Atlantic westerly winds, which in turn influences temperature and precipitation patterns in the Atlantic Northern Hemisphere (Hurrell 1995; Olsen et al. 2012; Patterson and Swindles 2015). The NAO and to a lesser extent AMO have been shown to have the most significant overall impact on winter climate in North America (Burakowski et al. 2010; Hubeny et al. 2006) The related AO is a measure of broader change in sea–level pressure of Arctic air masses in the Northern Hemisphere, of which the NAO is a localized constituent of (Deser 2000; Ambaum et al. 2001; Olsen et al. 2012; Young et al. 2012; Patterson and Swindles 2015). Both the AO and NAO have similar known influences on eastern North American weather during their positive (negative) phases, resulting in typically colder (warmer) temperatures, particularly during winter (Patterson and Swindles 2015; Yang et al. 2020). While both phenomena have relatively poorly defined frequencies, they typically range from subdecadal to interdecadal, and are occasionally characterized by 20+ year multidecadal oscillations (D'Arrigo et al. 2003; Olsen et al. 2012). Steinschneider and Brown (2011), Coleman and Budikova (2013), and Armstrong et al. (2014) have observed linkages between the NAO and hydroclimate variations in the eastern North America. Li et al. (2017) correlated intervals of persistent cold spells in eastern North America to the influence of the AO. Moreover, the AO is known to be associated with sea ice formation/melting in the Canadian Arctic (Rigor et al. 2002).

3.4 El Niño-Southern Oscillation (ENSO)

The ENSO originates in the equatorial Pacific where strengthening or weakening of equatorial trade winds in turn results in a strengthening or weakening of the upwelling of cold deep–ocean waters off the west coast of South America. This phenomenon has a far-reaching impact, influencing much of the world's climate with both its warm (El Niño) and cool (La Niña) phases (Ropelewski and Halpert 1986; Rodbell et al. 1999; Moy et al. 2002). In eastern North America, the influence of the ENSO is the result of the interaction of various atmospheric teleconnections (Bjerknes 1969; Diaz et al. 2001). Typically, only strong ENSO phases are reflected in weather patterns in eastern North America, leading to warmer, drier conditions during El Niño and cooler, wetter (snowier) conditions during La Niña, particularly in winter (Ropelewski and Halpert 1986; Harrison and Larkin 1998; Wolter et al.1999; Patterson and Swindles 2015; Yang et al. 2020).

3.5 Quasi-Biennial Oscillation (QBO)

The final major climate/weather driver considered here is the QBO, which is a measure of the variation between easterly and westerly winds in the equatorial stratosphere. The QBO record is typically

characterized by 2.1-2.2 and 2.3-2.4 year cycles, which have been shown to influence various aspects of near-surface climate via polar, subtropical, and tropical teleconnections (Gray et al. 2018). In eastern North America, the westerly phase of the QBO often leads to cooler surface temperatures, particularly in winter (Baldwin et al. 2001; Chattopadhyay and Bhatla 2002; Patterson and Swindles 2015). The QBO has also been shown to impact ice break-up in North American lakes (Sharma and Magnuson, 2014; Patterson and Swindles, 2015). The timing of lake ice break-up each year is primarily a function of late winter air temperatures, with other factors such as distance from coast, elevation, wind direction and wind intensity also being contributing factors (Patterson and Swindles, 2015).

Interactions between the cycles described above and their resultant influence on climate are well-documented. For example, AMO is known to weaken the effects of ENSO, NAO, and AO during its positive phase and amplify them during its negative phase (Zhang et al. 2012; Kang et al. 2014; Park and Li 2019; Zhang et al. 2019; Chen et al. 2020). Other climate oscillations thought to influence weather only weakly influence climate in the region, or occur with frequencies of hundreds or thousands of years, well beyond the instrumental records examined in this study (Mann et al. 1995; Domínguez-Villar et al. 2017).

Methods

4.1 Defining extreme weather

Various methods have been used to record and analyze extreme events (e.g. event counts or incremental classification; statistical, time series, and geospatial analysis; modelling), each tailored to differing approaches to what defines an extreme weather event (e.g. severe or unseasonal weather; weather at the limits of the historical distribution; e.g. Mondal and Mujumdar, 2015; Panda et al., 2016). Phenomena associated with the broad term “extreme weather event” can include, but are not limited to, rain or snowstorms, heat waves, cold snaps, droughts, floods, or hurricanes (Meehl et al. 2000; Stephenson et al. 2008; Huber and Gulledge 2011). Thus, a more specific definition of extreme weather in the context of this study is required. A common method for defining an extreme weather event is a statistical approach using the 95th percentile of historical climate data collected from a specific weather station or groups of stations (Rahmstorf and Coumou 2011; Gao et al. 2012). This concept can be simplified mathematically using the assumption that given aspects of weather (e.g. temperature, precipitation) follow a Gaussian distribution, with 95% of all weather events falling within two standard deviations of the mean ($\mu \pm 2\sigma$, where μ is the mean and σ is the standard deviation; Frei et al. 2015; Wang et al. 2015). Beyond these two standard deviations, weather events are considered extreme. This method uses univariate data (e.g. daily temperature records) and is only suitable for isolated extremes in that data (e.g. one day of abnormally high temperatures). Here, this method is employed for single day events and is not suitable if one wishes to recognize longer and/or less isolated events, such as hurricanes, the effects of which can last several days or weeks. While multi-day events can be recognized and analyzed using this approach, corrections must be applied to ensure multi-day events are mutually independent (Frei et al. 2015).

4.2 Data and analyses

Daily–resolution weather (temperature and precipitation) data was obtained from the historical data archives of Environment and Climate Change Canada and the National Oceanic and Atmospheric Association (NOAA) of the United States for 90 weather stations with long high-quality records from eastern North America (Fig. 1; stations listed in Appendix 1). The raw data spans various date ranges, typically beginning in the late 19th to early 20th centuries and continuing up to the 2010s, with the latest year analyzed being 2017. These 90 stations, which were distributed through the provinces of Ontario, Quebec, New Brunswick, Nova Scotia, and Prince Edward Island, and states of New York, Vermont, New Hampshire, Maine, Massachusetts, Connecticut, and Rhode Island, were subdivided using hierarchical agglomerative clustering (Sup. Fig. 1). Cluster analysis took into account the seasonal extreme weather event totals of each weather variable (maximum temperature, minimum temperature, rain, snow) for each given location, as well as latitude and longitude, using Ward's minimum variance linkage (Ward 1963). This approach resulted in recognition of three distinct climatic regions (informally designated as the Continental Region, Central Region, Maritime Region (MR), Sup. Fig. 1), which reflects the diversity of sub-climates found within this relatively large area of eastern North America.

This study focuses on the MR, which itself comprises distinct climatic subzones that are heavily influenced by proximity to the moderating influence of the Atlantic Ocean. Six stations within the MR were selected for detailed analysis based on the availability of long-running, high–quality climate records with no, or negligible missing data. They also provide a wide geographic distribution throughout the MR. These six locations are St. Margaret's Bay, NS (1922 – 2018), Annapolis Royal (1915 – 2007), NS, Moncton, NB (1881 – 2018), Nepisiguit Falls, NB (1922 – 2006), Causapscal, QC (1913 – 2018), and Houlton, ME (1902 – 2013; Fig. 1).

MATLAB (MathWorks 2019) was used to separate each record by meteorological season (December–February, March–May, June–August, September–November). The means and standard deviations for temperature (high, low) and precipitation (snow, rain) were calculated for these four seasons for the entirety of the available weather records. For precipitation, means and standard deviations were only calculated for non–zero values, as days with zero precipitation values would unfavourably skew the data. Temperature and precipitation values that fell outside of two standard deviations from the mean (the 95th percentile) were considered extreme. The number of extreme events for each season and year were tallied for further analysis.

The variability of extreme weather events through time was analyzed by calculating linear best fits as well as by red noise spectral and wavelet time series analyses. Spectral and wavelet time series analysis provide complementary results. Spectral analysis provides a very good estimate of signal periodicity but presumes stationarity, while non-stationary wavelet analysis provides an indication of the distribution and interrelationship of signals with varying frequencies through time (Prokoph and Patterson 2004). Red noise spectral analysis, a function based on Thomson's multitaper method (Dorothée 2020), was used to transform time–domain data into its frequency domain counterpart. As opposed to a basic

Fourier transform, which provides a single spectral power estimate, this method utilizes several estimates of a power spectrum and averages them, eliminating potential biases that can arise when using a simple Fourier transform (Thomson 1982). Red noise and confidence levels were estimated using the Monte Carlo and chi-square methods (Schulz and Mudelsee 2002). Typically, a 95% confidence interval is used to validate statistically viable periodic trends, though slightly lower confidence intervals remain statistically significant. Confidence levels of 90% and 99% are also often used in statistical analysis. Here, any periodic signals above the 90% confidence interval were considered significant, as this level still maintains data robustness (Zar 1998). Continuous wavelet transforms (CWTs) were applied to the extreme weather records, presenting the spectral information with the additional element of time, which provides information on the continuous or discontinuous nature of the periodic signals.

Cross wavelet transforms (XWT) were then carried out between the various extreme weather records and the six climate oscillations discussed in Section 3 (SSC (SILSO, 2021), AMO (Trenberth et al. 2021), AO (NCAR 2021), NAO (Hurrell and NCAR 2020), ENSO (Trenberth and NCAR 2020) and QBO (NCAR 2013)) using the MATLAB functions by Grinsted et al. (2004), yielding comparisons between the extreme weather records and climate oscillations. While a CWT is useful to analyze a single time series for oscillatory components, an XWT can be constructed to reveal the common spectral power between two time series (i.e. exposing the oscillatory components that both time series share at a given point in time; Grinsted et al. 2004). This transform is particularly useful for assessing the relationship between two cyclic time series, providing a visual representation of statistically significant correlated oscillations between two data sets. The XWT scalograms indicate the 95% confidence interval of statistically significant common oscillations (shown as areas of high spectral density outlined with a solid black line). The XWT analyses were carried out to assess the relationships that the various aspects of extreme weather have to various climate oscillations.

Results

5.1 Linear regressions

The seasonal linear regressions for each intra-station extreme weather variable are typically characterized by near-zero to very shallow positive or negative slopes depending on the season and weather variable (-1.78–0.79 events/100 years; Sup. Fig. 1–4, Sup. Table 1). The shallowness of the slopes and variability in sign across the region indicates that there has been no consistent, long-term, regional trend in the periodicity of extreme weather phenomena in the timeframe spanned by the MR instrumental record. However, there do appear to be several trends in the periodicity of extreme weather events that are unique to individual or small groupings of climate stations.

In general, there has been an increase in regional seasonal variability of extreme rainfall events with notably consistent seasonal increases in extreme rainfall events in Houlton, ME and Moncton, NB. There has also been a consistent increase in extreme snowfall events in Moncton. The remaining stations display near-zero trends in extreme snowfall.

The maximum extreme weather slope observed was 2.37 events/100 years (summer rain, Houlton) and the minimum observed slope was -4.07 events/100 years (summer minimum temperature, Nepisiguit Falls, NB). The majority (70.8%) of the linear regressions fall between -1 – 1 event/100 years, 85.4% fall between -1.5 and +1.5 events/100 years, and 90.6% of events fall between -2 and +2 events/ 100 years. Four of these larger changes were correlated to summer extreme weather records, and three of these occurred at Nepisiguit Falls, which is characterized by the strongest weather linear trends of any of the studied stations. Nepisiguit Falls is experiencing declines in both extreme maximum and minimum temperature events for a given season, indicative of a narrowing of local climate variability (Sup. Fig. 1-4, Sup. Table 1).

For extreme maximum temperature events the St. Margaret's Bay, NS, station has been characterized by consistently positive slopes, whereas the extreme minimum temperatures recorded for the same station display consistently negative slopes. This step-wise increase in extreme warm temperatures and decrease in cold temperatures is consistent with a progressively warming local climate at St. Margaret's Bay.

5.2 Spectral analysis and wavelet transforms

Spectral analysis and CWTs display many statistically significant cycles at the 90% confidence interval and higher throughout the MR (Figs. 2–9). Across the six stations, there was variation in the observed cycles within each of the seasonal weather records, although regional trends and spatial gradients were observed between stations. Extreme maximum and minimum temperature data exhibited 2.8–3.2 year non-stationary cycles spanning all the seasons at nearly all stations (Figs. 2–3 and 6–7). This cyclicity is particularly strong at all stations for 1997–2000 autumn extreme maximum temperature (Fig. 6). Similarly, a 2.8 year cycle occurred during summer in the mid–1940s at all stations except for St. Margaret's Bay and Annapolis Royal, NS. Other cycles in extreme maximum temperature that can be seen across several, or all stations, are 5.1–6.6 years (spring, 1970s), 9–11 years (spring, 1940–1960), and 3.2–4 years (winter, 1940s). Cycles observed for extreme minimum temperature across nearly all stations include: ~3.7 years (autumn, 1980s); 3.2–4.2 years (autumn, 1930s); 2.8–3.3 years (summer, ~2000); 5.1–5.7 years (spring, ~1940); and 3.9–5.3 years (winter, 1930s and 1960s).

Most stations are also characterized by statistically significant non-stationary extreme rain and snow precipitation cycles of 2–3 years across all seasons (Figs. 4–5 and 8–9). However, these cycles are not quite as well correlated across the entire region as was the case for extreme temperature.

There were non-stationary 3.4–3.7 year extreme rainfall cycles (spring, 1990s) observed at all stations, although this cycle was only statistically significant at some stations. There was also a 9.5–11 year non-stationary cycle (winter, 1970s– 1990s) and ~3 years (spring, 1910s) observed at Houlton and Moncton. The records at these two stations also included non-stationary 3.1–3.2 year cycles in extreme snowfall (spring, ~2000). There was also a 2–3 year snowfall cycle (autumn, 1950s) present only at St. Margaret's Bay and Annapolis Royal.

Regional variation in MR precipitation cycles reflects the influence of the Atlantic Ocean. The weather at stations in more coastal environments (St. Margaret's Bay and Annapolis Royal, NS) typically receive more precipitation as rainfall throughout the year, as well as being more likely to be impacted by the remnants of tropical storms than the inland stations. These two coastal stations have similar extreme precipitation records, quite distinct from the records from the other stations. More inland, continental-weather-influenced Houlton and Moncton are also more similar to one another for the same reason.

5.3 Cross wavelet transforms

The XWTs facilitate direct comparison of the documented extreme temperature and precipitation weather records with the published SSC, AMO, NAO, AO, ENSO, and QBO time series datasets (NCAR 2013, 2020; Hurrell and NCAR 2020; Trenberth and NCAR 2020; Trenberth et al. 2021; SILSO 2021) by identifying frequencies that any two time series under investigation (e.g. a regional climate driver and an extreme weather record) have in common at a given time. The results of the XWT comparison between the SSC, AMO, NAO, AO, ENSO, and QBO and Annapolis Royal maximum temperature and Moncton rainfall are presented in Figs. 10 and 11, respectively. These two example climate stations were chosen to highlight as they are representative of the relationship between these various climate patterns and rainfall and maximum temperature throughout the entire region. The XWT results between the extreme rainfall, snowfall, and high and low temperatures for all stations and each of the SSC, AMO, NAO, AO, ENSO, and QBO phenomena are presented in Sup. Figs. 5–29.

The strongest observed relationship between the extreme temperature and precipitation data and cyclic climate drivers was an ~ 11 year cycle that correlates with the SSC (Sup. Figs. 5–9). This strong relationship with the SSC included all stations and all extreme weather types analyzed, and although non-stationary, in most cases extended throughout the entire instrumental record. Examples of non-stationarity included a discontinuity between the SSC and maximum temperature in summer (~1960–1980) Moncton, Houlton, and St. Margaret's Bay, as well as during autumn (~1930–1950 and ~1970–1985) in St. Margaret's Bay and Annapolis Royal. Similar discontinuities were recognized in the SSC-extreme minimum temperature relationship. The Causapscal, QC, and Nepisiguit Falls stations also display non-stationarity in the relationships between extreme temperatures and the SSC, though to a lesser degree. Extreme precipitation shows the highest degree of continuity in common spectral power with the SSC across the region.

The XWTs for AMO and each of the extreme weather variables (Sup. Figs. 10–13) were characterized by many small areas of weak common spectral power, although with extreme temperature and precipitation there was for many stations an area of high common power with a cycle of ~16–30 years, typically centered upon ~1950. This relationship was most apparent with winter and summer maximum temperature, summer minimum temperature and winter snowfall and was variable by location with

rainfall, appearing most strongly in the coastal stations, St. Margaret's Bay and Annapolis Royal. Several occurrences of common ~4 and ~8 year cycles were also observed.

The XWTs for both the NAO (Sup. Figs. 14–17) and AO versus each extreme weather variable (Sup. Figs. 18–21) indicate that these drivers have had a varying impact on extreme high and low temperatures across the region, with many intermittent occurrences of common cycles ranging from 2 – 16 years. The climatic influence of NAO across the region varies considerably between stations, with relatively few, and typically weak regional patterns. In contrast the XWTs between extreme precipitation and AO indicates that an abrupt climatic shift occurring around ~1965 for all stations, although prior to this part of the regional record the common spectral power between extreme precipitation and AO is sparse and weak. During the post–1965 interval, this relationship became stronger, with higher common spectral power between the signals. This shift is not as clear when AO is compared to extreme temperatures, though a clear regional pattern exists. While NAO does not show the time-varying pattern that the AO does, many of the strongest common cycles between extreme weather and NAO are similar to those shown with the AO.

The ENSO-extreme weather XWT results (Sup. Figs. 22–25) are broadly similar to those patterns observed for the NAO and AO XWTs. In particular, the XWTs for ENSO and temperature extremes are strongly correlated between stations, with extreme precipitation showing an abrupt change in common spectral power beginning in ~1965, as occurred in the AO results. As observed with AO, areas of high common spectral density increased post–1965, although this trend is less pronounced. The abrupt shift correlated to ENSO is also apparent across the region with the winter and spring rainfall and spring snowfall extremes. The high and low frequency signals within the NAO, AO, and ENSO XWTs show distinct similarities to the resulting AMO XWTs, suggesting a relationship between the effects of these four phenomena and their influence on extreme weather.

Each of the ENSO, NAO, and AO versus extreme weather XWTs are also characterized by a relatively strong 16–30+ year common cycle with various extreme weather records (e.g. winter maximum temperature – AO, Annapolis Royal (Sup. Fig. 18); summer minimum temperature – NAO, Moncton (Sup. Fig. 15)), reminiscent of the relationships found between extreme temperature and the AMO. This is most often found during winter, but these relationships are present in other seasons as well.

The QBO versus extreme weather XWT results (Sup. Figs. 26–29) indicate that this driver has had a pulsed non-stationary influence on extreme weather throughout the MR with the most significant influence being on extreme precipitation, and less so on extreme temperature. The QBO XWT data is strongly correlated across the region with the notable exception of the Annapolis Royal station. With extreme maximum temperature, QBO has had a stronger influence during winter, and has been weakest during summer. The relationship between QBO and extreme minimum temperature, is fairly uniform regardless of the season. The most common XWT periodicity observed with temperature has primarily been in the 2–3 year range, although particularly with extreme maximum temperature there is a semi–consistent 10–20 year cyclicity that spans from the beginning of the QBO record (1953) to 1980. This 10-

20 cycle is even more strongly expressed with extreme precipitation, with the 2–3 year cycles described above still present.

Discussion

6.1 Maritime Region (MR) extreme weather trends

Weather patterns in the MR of eastern North America are significantly influenced by its proximity to the Atlantic Ocean, which moderates the climate there, particularly in coastal areas. However, areas only a few kilometres inland are significantly influenced by continental climate conditions (Trewartha and Horn 1980; Patterson and Swindles 2015). For example, in summer the Atlantic coast is often shrouded in fog with temperatures of < 20°C, while it may be sunny and >30°C only a few km inland. Then in winter the coast may be snow free and rainy while areas only a short distance from the coast may be covered in a thick blanket of snow. Thus, considering the spatial distribution of weather stations used in this study, a gradient in climatic trends is fully expected. The gradient in climatic conditions was most significant between the two most coastal weather stations, St. Margaret's Bay and Annapolis Royal, and the remaining four stations, which are characterized by more continental climates (e.g. Fig. 7, Sup. Fig. 10). Of the inland stations the climatic patterns characterizing Moncton and Houlton were most similar to each other, most likely related to the close latitudinal positioning of the stations at 46.09°N and 46.13°N, respectively. These results suggest that even at the small regional scale studied, latitudinal climate gradients impact the periodicity of extreme weather occurrences.

6.2 Linear trends in extreme weather events

Nearly all of the extreme weather records for the MR are, based on regression analysis results, characterized by fairly shallow slopes, with only relatively small changes, both positive and negative, in the periodicity of extreme weather through the past ~100 years, with little spatial coherence. There were nine weather records in the region though that exceeded an increase/decrease threshold of 2 events/100 years. These records were primarily concentrated in the minimum temperature extremes, particularly for Nepisiguit Falls and Annapolis Royal (Sup. Table 1). With the vast majority of linear regressions in the extreme precipitation and temperature records for the MR being negligible through the span of the instrumental data record examined, the confounding influence of natural climatic oscillations further complicate detection of any trajectory in these records. These results, at least for the MR, contrast with some recently published studies, which report that extreme weather events are becoming more frequent as global temperatures continue to rise (Perkins-Kirkpatrick et al. 2017; Francis et al. 2018; Keellings et al. 2018; Cowan et al. 2020; Perkins-Kirkpatrick and Lewis 2020).

6.3 Influence of Cyclic Climate teleconnections

6.3.1 Schwabe solar cycle (SSC)

The prominent 9–12 year cycles that recurs throughout the extreme weather data for the MR, and the strong common periodicity in this range between extreme weather and the SSC observed in the XWT analysis results, indicates that this phenomenon is the most significant influence on each aspect of climate analyzed in the region (Sup. Fig. 5-9).

The observed linkage between MR extreme weather records to the SSC is similar to the findings of Laurenz et al. (2019), where the SSC was found to correlate with European rainfall totals. However, in that study it was observed that there was a moderate month to month correlation between variation in the strength of solar influence on extreme precipitation, which in contrast to the results for the MR, were significantly reduced at the seasonal level. The wider geographic coverage, accompanied by a wider regional climatic variability, used by Laurenz et al. (2019) may explain the greater month to month variation between the two studies.

Additionally, Prokoph et al. (2012) attributed an ~11-year cycle in MR steam flow records to the SSC, although they also noted that this signal was comparably weaker than what was observed in rivers elsewhere in Canada. Moreover, the SSC is known to influence other natural cyclic climate phenomena (e.g. QBO and ENSO (Quiroz 1981; Hamilton 2002; Kuroda 2007; Fischer and Tung 2008; Calvo and Marsh 2011; Zhou et al. 2013)), which could possibly explain the observed non-stationary relationship between the SSC and extreme weather in the MR, particularly the relationship with extreme minimum temperature.

6.3.2 Atlantic Multidecadal Oscillation

The XWTs comparing the AMO index and MR extreme weather data revealed a common ~16–30 year cycle recognizable in varying degrees in both temperature and precipitation data, which was widespread across the region between 1930 and 1970. This period range corresponds to a suspected subharmonic influence of the AMO on this region; 16-24 year subharmonics of the AMO have been reported by Ruiz-Barradas et al. (2013) and have been found to influence climatic trends in the MR, particularly those related to temperature fluctuations, by Patterson and Swindles (2015). Furthermore, this 1930 – 1970 interval, corresponding to a positive phase of the AMO, was most common in extreme temperatures and snowfall data from Nova Scotia stations, although extreme rainfall data also was characterized by this pattern, albeit with a weaker spectral power. While this effect was observed most strongly in the Nova Scotia stations, it appeared more weakly in the remaining MR stations, indicating a coastal-inland effect of the AMO in this region. This gradational effect can be seen in both extreme temperature/AMO XWTs

(Sup. Figs. 10, 11), in which the coastal Nova Scotia stations experience the strongest relationships, particularly in winter months.

6.3.3 NAO, AO, and ENSO

Several parallels were observed in the relationships between NAO, AO, and ENSO XWT results. Each of these oscillations exhibited common cycles of 2–16 years that appeared at similar times between the three oscillations. Furthermore, both ENSO and AO exhibited a shift from low common spectral power to high common spectral power at ~1965. These patterns suggest the NAO, AO, and ENSO share an interactive influence on extreme weather in the MR.

From the XWT results, both ENSO and AO have a relatively uniform influence on extreme weather across the MR, with similar signals observed across all stations for a given season and weather type. In particular, ENSO has the most significant influence over extreme temperatures in the MR, particularly in winter and spring (Sup. Fig. 22-23). ENSO and AO collectively have a similar but more moderate influence on extreme precipitation (Sup. Fig. 24-25, Sup. Fig. 20-21), with the NAO having a comparatively weaker influence on this parameter. In contrast to ENSO and AO, the influence of the NAO often has a higher spatial variation with respect to extreme weather throughout the MR (Sup. Fig. 14-17).

There is a notable common 16–30 year cycle observed in the XWT extreme temperature records for the NAO, AO, and ENSO, particularly during winter. These lower frequency cycles parallel similar XWT results observed with the AMO data. In addition, ~4 and ~8 year XWT links between the AMO and extreme weather records also parallel many of the significant relationships observed with the XWT derived correlations between extreme weather and ENSO, NAO, and AO. These resemblances suggest a strong interaction and significant modulation of ENSO, NAO, and AO by the AMO in the MR (e.g. Fig. 10 displays stark similarities between the maximum temperature XWT analyses for AMO, NAO, AO, and ENSO at Annapolis Royal, NS).

The interrelationship between AMO, NAO, AO, and ENSO is particularly strong in coastal areas, particularly in the respective extreme temperature XWTs. For example, the extreme maximum temperature record from Annapolis Royal record is characterized by a close similarity observed within each season between each of these four climate oscillations (Fig. 10). This close relationship between these oscillations is also observed at many inland stations, albeit generally less strongly (e.g. Moncton extreme rainfall, Fig. 11). This same pattern is also weakly observable in the extreme precipitation XWTs, although it is much more variable.

In the MR, this influence was further supported by observed patterns within the AO–extreme precipitation XWTs. For example, the common periodicity between AO and extreme precipitation became amplified after 1965 following the establishment of an AMO- phase. A similar post–1965 amplification was

observed in the ENSO XWT record, although these effects were more varied by season and weather type. The significant influence of the AMO in modulating the effects of other cyclic climate phenomena (such as the NAO, AO, and ENSO) has also been previously documented elsewhere in North America, where it has been observed that this phenomenon suppresses the influence of their effects during an AMO+ phase and amplifying them during an AMO- phase (Mo et al. 2009; Zhang et al. 2012; Kang et al. 2014; Park and Li 2019; Zhang et al. 2019).

6.3.4 The Quasi-Biennial Oscillation

In the MR the influence of the QBO appeared strongest within the extreme precipitation record (both rain and snow) and was weakest within the extreme minimum temperature record. This result is partially contradictory to the spectral analysis results, where 2–3 year cycles appeared in nearly all extreme temperature records and, less commonly in the extreme precipitation records. A possible explanation for the discrepancy is that there is probable overlap between lower frequency QBO and higher frequency ENSO signals. This strong observed correlation between QBO and fluctuations in extreme rainfall and snowfall patterns is also supported by research from elsewhere in North America and around the globe (Lau and Sheu, 1988; Brázdil Zolotokrylin 1995; Inoue and Yamakawa 2010; Seo et al. 2013). Similarly, several extreme rainfall records have been found to be characterized by quasi-biennial patterns, although in many cases they have not necessarily being linked to the QBO (Nastos and Zerefos 2007; Becker et al. 2008; Han et al. 2020).

The lower–frequency cycles observed in many of the QBO XWTs from 1953–1980 (e.g. Fig. 10, QBO row) are likely a result of modulation of what has been dubbed the quasi–decadal oscillation, which has been attributed to influence of the SSC (e.g. Quiroz,1981; Hamilton, 2002; Fischer and Tung, 2008). It is hypothesized that changes in TSI through the 11-year SSC influences movement of upper stratospheric air masses, where there are also strong SSC-linked changes in solar–ozone radiative forcing. Overprinting on the QBO signal results in a quasi–decadal trend within in the QBO index. In the MR this modulation is seen most strongly in the pre-early 1980s QBO.

Conclusions

Through implementation of spectral, Morlet wavelet and cross wavelet analysis we have demonstrated that the occurrence of extreme weather (precipitation (snow, rain) and temperature (high, low)) in the instrumental record (~100-150 years) from six climate stations in the MR of eastern North America is largely cyclical, showing only localized evidence of either negative or positive trends. A regional gradation in extreme weather occurrence is recognizable when comparing coastal and inland/continental areas. It was found that the observed cyclic components of seasonal extreme weather are principally driven by several natural climate oscillations, the strongest of which is the ~11-year SSC. The SSC cycle exhibited

both continuous and discontinuous impact through time in all seasons on the occurrence of extreme maximum and minimum temperature, rainfall, and snowfall.

Other cycles found to influence the occurrence of extreme weather were the AMO, NAO, AO, ENSO, and QBO. The influence of NAO, AO, and ENSO on extreme weather were modulated by negative and positive phases of the AMO, with distinct similarities between the four oscillations that would otherwise be unexpected. In particular the negative phase of the AMO appears to amplify the impacts of the AO and ENSO. Moreover, comparison of the AMO, NAO, AO, and ENSO records with extreme weather records in the MR indicates that there seems to be a complex interplay between them that causes some uniformity in their influence, particularly on extreme temperature events through the 20th and early 21st centuries for a given station.

The QBO had a frequent but discontinuous impact on extreme weather in the MR through time, having a stronger relationship with extreme precipitation than extreme temperature. Furthermore, there was a modulating effect of the SSC on the QBO spanning from the 1950s to the 1980s, which was reflected in the XWT analysis for most stations in the MR.

References

Ambaum, M. H., Hoskins, B. J., and Stephenson, D. B. (2001). Arctic oscillation or North Atlantic oscillation? *J Clim*, 14(16):3495–3507.

Ananthakrishnan, R. and Parthasarathy, B. (1984). Indian rainfall in relation to the sunspot cycle: 1871–1978. *J Climatol*, 4(2):149–169.

Andalo, C., Beaulieu, J., and Bousquet, J. (2005). The impact of climate change on growth of local white spruce populations in Quebec, Canada. *For Ecol Manag*, 205(1-3):169–182.

Andrey, J., Mills, B., Leahy, M., and Suggett, J. (2003). Weather as a chronic hazard for road transportation in Canadian cities. *Nat Hazards*, 28(2-3):319–343.

Armstrong, W. H., Collins, M. J., and Snyder, N. P. (2014). Hydroclimatic flood trends in the northeastern United States and linkages with large-scale atmospheric circulation patterns. *Hydrol Sci J*, 59(9):1636–1655.

Balbus, J. M. and Malina, C. (2009). Identifying vulnerable subpopulations for climate change health effects in the United States. *J Occup Environ Med*, 51(1):33–37.

Baldwin, M., Gray, L., Dunkerton, T., Hamilton, K., Haynes, P., Randel, W., Holton, J., Alexander, M., Hirota, I., Horinouchi, T., et al. (2001). The quasi-biennial oscillation. *Rev Geophys*, 39(2):179–229.

Becker, S., Hartmann, H., Coulibaly, M., Zhang, Q., and Jiang, T. (2008). Quasi periodicities of extreme precipitation events in the Yangtze River basin, China. *Theor Appl Climatol*, 94(3-4):139–152.

Bjerknes, J. (1969). Atmospheric teleconnections from the equatorial Pacific. *Mon Weather Rev*, 97(3):163–172.

Boland, G., Melzer, M., Hopkin, A., Higgins, V., and Nassuth, A. (2004). Climate change and plant diseases in Ontario. *Can J Plant Pathol*, 26(3):335–350.

Bonsal, B. and Shabbar, A. (2011). *Large-scale climate oscillations influencing Canada, 1900-2008*. Canadian Councils of Resource Ministers.

Bonsal, B., Zhang, X., Vincent, L., and Hogg, W. (2001). Characteristics of daily and extreme temperatures over Canada. *J Clim*, 14(9):1959-1976.

Bouwer, L.M., 2019. Observed and projected impacts from extreme weather events: implications for loss and damage. In *Loss and damage from climate change* (pp. 63-82). Springer, Cham.

Brázdil, R. and Zolotokrylin, A. (1995). The QBO signal in monthly precipitation fields over Europe. *Theor Appl Climatol*, 51(1-2):3–12.

Burakowski EA, Braswell RH, Wake CP, Bradbury J, Brown DP (2010) Influence of NAO, ENSO, and AMO on northeast US winter temperatures and snow cover: 1949–2005. Carbon Solutions New England report, p 12

Calvo, N. and Marsh, D. R. (2011). The combined effects of ENSO and the 11 year solar cycle on the Northern Hemisphere polar stratosphere. *J Geophys Res: Atmos*, 116(D23).

Chattopadhyay, J. and Bhatla, R. (2002). Possible influence of QBO on teleconnections relating Indian summer monsoon rainfall and sea-surface temperature anomalies across the equatorial pacific. *Int J Clim*, 22(1):121–127.

Chen, S., Chen, W., Wu, R., and Song, L. (2020). Impacts of the Atlantic Multidecadal Oscillation on the spring Arctic Oscillation-following East Asian summer monsoon relation. *J Clim*.

Cheng, C. S., Auld, H., Li, Q., and Li, G. (2012). Possible impacts of climate change on extreme weather events at local scale in south–central Canada. *Clim Change*, 112(3-4):963–979.

Cohen, J., Screen, J. A., Furtado, J. C., Barlow, M., Whittleston, D., Coumou, D., Francis, J., Dethloff, K., Entekhabi, D., Overland, J., et al. (2014). Recent Arctic amplification and extreme mid-latitude weather. *Nature Geosci*, 7(9):627.

Coleman, J. S. and Budikova, D. (2013). Eastern US summer streamflow during extreme phases of the North Atlantic Oscillation. *J Geophys Res: Atmos*, 118(10):4181–4193.

Cowan, T., Undorf, S., Hegerl, G. C., Harrington, L. J., and Otto, F. E. (2020). Present day greenhouse gases could cause more frequent and longer Dust Bowl heatwaves. *Nature Clim Change*, pages 1–6.

Currie, R. G. (1993). Luni-solar 18.6-and solar cycle 10–11-year signals in USA air temperature records. *Int J Clim*, 13(1):31–50.

Currie, R. G. and O'Brien, D. P. (1988). Periodic 18.6-year and cyclic 10 to 11 year signals in northeastern United States precipitation data. *J Climatol*, 8(3):255–281.

Currie, R. G. and Vines, R. G. (1996). Evidence for luni–solar and solar cycle signals in Australian rainfall data. *Int J Clim*, 16(11):1243–1265.

D'Arrigo, R. D., Cook, E. R., Mann, M. E., and Jacoby, G. C. (2003). Tree-ring reconstructions of temperature and sea-level pressure variability associated with the warm-season Arctic Oscillation since AD 1650. *Geophys Res Lett*, 30(11).

Deser, C. (2000). On the teleconnectivity of the "Arctic Oscillation". *Geophys Res Lett*, 27(6):779–782.

Diaz, H. F., Hoerling, M. P., and Eischeid, J. K. (2001). ENSO variability, teleconnections and climate change. *Int J Clim*, 21(15):1845–1862.

Dima, M. and Lohmann, G. (2007). A hemispheric mechanism for the Atlantic Multidecadal Oscillation. *J Clim*, 20(11):2706–2719.

Dolney, T. J. and Sheridan, S. C. (2006). The relationship between extreme heat and ambulance response calls for the city of Toronto, Ontario, Canada. *Environ Res*, 101(1):94–103.

Domínguez-Villar, D., Wang, X., Krklec, K., Cheng, H., & Edwards, R. L. (2017). The control of the tropical North Atlantic on Holocene millennial climate oscillations. *Geology*, *45*(4), 303-306.

Dorothée (2020). Red Noise Confidence Levels (https://www.mathworks.com/matlabcentral/fileexchange/45539-rednoise_confidencelevels). *MATLAB Central File Exchange*, retrieved February 11, 2020.

Douglas, E. M. and Fairbank, C. A. (2010). Is precipitation in northern New England becoming more extreme? Statistical analysis of extreme rainfall in Massachusetts, New Hampshire, and Maine and updated estimates of the 100-year storm. *J Hydrol Eng*, 16(3):203–217.

Du, J., Wang, K., Wang, J., and Ma, Q. (2017). Contributions of surface solar radiation and precipitation to the spatiotemporal patterns of surface and air warming in China from 1960 to 2003. *Atmos Chem Phys*, 17(8).

Enfield, D. B. and Cid-Serrano, L. (2010). Secular and multidecadal warmings in the North Atlantic and their relationships with major hurricane activity. *Int J Clim*, 30(2):174– 184.

Enfield, D. B., Mestas-Nun˜ez, A. M., and Trimble, P. J. (2001). The Atlantic Multidecadal Oscillation and its relation to rainfall and river flows in the continental us. *Geophys Res Lett*, 28(10):2077–2080.

Fischer, P. and Tung, K. (2008). A re-examination of the QBO period modulation by the solar cycle. *J Geophys Res: Atmos*, 113(D7).

Francis, J., Skific, N., and Vavrus, S. (2018). North American weather regimes are becoming more persistent: Is Arctic amplification a factor? *Geophys Res Lett*, 45(20):11–414.

Frei, A., Kunkel, K. E., and Matonse, A. (2015). The seasonal nature of extreme hydrological events in the northeastern United States. *J Hydrometeorol*, 16(5):2065–2085.

Gao, Y., Fu, J. S., Drake, J., Liu, Y., and Lamarque, J.-F. (2012). Projected changes of extreme weather events in the eastern United States based on a high resolution climate modeling system. *Environ Res Lett*, 7(4):044025.

Gray, L.J., Beer J., Geller, M., Haigh, J.D., Lockwood, M., Matthes, K., Cubasch, U., Fleitmann, D., Harrison, G., Hood, L., Luterbacher, J., Meehl, G.A., Shindell, D., van Geel, B. White, W. (2010). Solar influences on climate. *Rev Geophys*, 48:RG4001.

Gray, L. J., Anstey, J. A., Kawatani, Y., Lu, H., Osprey, S., and Schenzinger, V. (2018). Surface impacts of the Quasi Biennial Oscillation. *Atmos Chem Phys*, 18(11):8227–8247.

Grinsted, A., Moore, J. C., and Jevrejeva, S. (2004). Application of the cross wavelet transform and wavelet coherence to geophysical time series. *Nonlinear Proc Geophys*, 11(5/6):561–566.

Hamilton, K. (2002). On the quasi-decadal modulation of the stratospheric QBO period. *J Clim*, 15(17):2562–2565.

Hathaway, D. H. (2010). The Solar Cycle. *Living Rev Sol Phys*, 7(1):2367– 3648.

Han, T., Li, S., Hao, X., and Guo, X. (2020). A statistical prediction model for summer extreme precipitation days over the northern central China. *Int J Clim*, 40(9):4189–4202.

Harrison, D. and Larkin, N. (1998). Seasonal US temperature and precipitation anomalies associated with El Nin˜o: Historical results and comparison with 1997-98. *Geophys Res Lett*, 25(21):3959–3962.

Hathaway, D. H. (2015). The Solar Cycle. *Living Rev Sol Phys*, 12(1):4.

Hubeny JB, King JW, Santos A (2006) Subdecadal to multidecadal cycles of Late Holocene North Atlantic climate variability preserved by estuarine fossil pigments. Geology 34:569–572

Huber, D. G. and Gulledge, J. (2011). *Extreme weather and climate change: Understanding the link, managing the risk*. Pew Center on Global Climate Change Arlington.

Hurrell, J. W. (1995). Decadal trends in the North Atlantic Oscillation: regional temperatures and precipitation. *Science*, 269(5224):676–679.

Hurrell, James & National Center for Atmospheric Research (NCAR) Staff (Eds). (2020). *The Climate Data Guide: Hurrell North Atlantic Oscillation (NAO) Index (station-based).* Retrieved from https://climatedataguide.ucar.edu/climate-data/hurrell-north-atlantic-oscillation-nao-index-station-based

Inoue, M. and Yamakawa, S. (2010). Relationships between Stratospheric Quasi-Biennial Oscillation (QBO). *J Geog*, 119(3):441–450.

Jørgensen, C. S., Karoff, C., Pavai, V. S., and Arlt, R. (2019). Christian Horrebow's sunspot observations–I. Life and published writings. *Sol Phys*, 294(6):77.

Kang, I.-S., No, H.-h., and Kucharski, F. (2014). ENSO amplitude modulation associated with the mean SST changes in the tropical central Pacific induced by Atlantic Multidecadal Oscillation. *J Clim*, 27(20):7911–7920.

Keellings, D., Bunting, E., and Engström, J. (2018). Spatiotemporal changes in the size and shape of heat waves over North America. *Clim Change*, 147(1-2):165–178.

Knight, J. R., Folland, C. K., and Scaife, A. A. (2006). Climate impacts of the Atlantic multidecadal oscillation. *Geophys Res Lett*, 33(17).

Knudsen, M. F., Seidenkrantz, M.-S., Jacobsen, B. H., and Kuijpers, A. (2011). Tracking the Atlantic Multidecadal Oscillation through the last 8,000 years. *Nature Commun*, 2(1):1–8.

Kuroda, Y. (2007). Effect of QBO and ENSO on the solar cycle modulation of winter North Atlantic Oscillation. *J Meteorol Soc Jpn. Ser. II*, 85(6):889–898.

Lassen, K. and Friis-Christensen, E. (1995). Variability of the solar cycle length during the past five centuries and the apparent association with terrestrial climate. *J Atmos Terr Phys*, 57(8):835–845.

Lau, K.-M. and Sheu, P. (1988). Annual cycle, Quasi-Biennial Oscillation, and Southern Oscillation in global precipitation. *J Geophys Res: Atmos*, 93(D9):10975–10988.

Laurenz, L., Lüdecke, H.-J., and Lüning, S. (2019). Influence of solar activity changes on European rainfall. *J Atmos Sol Terr Phys*, 185:29– 42.

Lemieux, C. J. and Scott, D. J. (2011). Changing climate, challenging choices: identifying and evaluating climate change adaptation options for protected areas management in Ontario, Canada. *Environ Manag*, 48(4):675.

Li, F., Orsolini, Y. J., Wang, H., Gao, Y., and He, S. (2018). Atlantic Multidecadal Oscillation modulates the impacts of Arctic sea ice decline. *Geophys Res Lett,* 45(5):2497–2506.

Li, Z., Manson, A. H., Li, Y., and Meek, C. (2017). Circulation characteristics of persistent cold spells in central–eastern North America. *J Meteorol Res,* 31(1):250–260.

Linnenluecke, M. K., Griffiths, A., and Winn, M. (2012). Extreme weather events and the critical importance of anticipatory adaptation and organizational resilience in responding to impacts. *Bus Strategy Environ*, 21(1):17–32.

Liu, Y. (2014). Estimation and uncertainty analysis of impacts of future heat waves on mortality in the eastern United States. *Environ Health Perspect*, 122(1):10–16.

Lockwood, M. (2012). Solar influence on global and regional climates. *Surv Geophys*, 33(3-4):503–534.

Maliniemi, V., Asikainen, T., and Mursula, K. (2014). Spatial distribution of Northern Hemisphere winter temperatures during different phases of the solar cycle. *J Geophys Res: Atmos*, 119(16):9752–9764.

MathWorks (2019). *MATLAB Version 9.6.0.10 (R2019a)*. The MathWorks Inc., Natick, Massachusetts.

Mazzarella, A. and Palumbo, F. (1992). Rainfall fluctuations over Italy and their association with solar activity. *Theor Appl Climatol*, 45(3):201–207.

Meehl, G. A. and Arblaster, J. M. (2009). A lagged warm event–like response to peaks in solar forcing in the Pacific region. *J Clim*, 22(13):3647–3660.

Meehl, G. A., Arblaster, J. M., Matthes, K., Sassi, F., and van Loon, H. (2009). Amplifying the Pacific climate system response to a small 11-year solar cycle forcing. *Science*, 325(5944):1114–1118.

Meehl, G. A., Karl, T., Easterling, D. R., Changnon, S., Pielke Jr, R., Changnon, D., Evans, J., Groisman, P. Y., Knutson, T. R., Kunkel, K. E., et al. (2000). An introduction to trends in extreme weather and climate events: observations, socioeconomic impacts, terrestrial ecological impacts, and model projections. *Bull Am Meteorol Soc*, 81(3):413–416.

Mendoza, B., Lara, A., Maravilla, D., and Ja´uregui, E. (2001). Temperature variability in central Mexico and its possible association to solar activity. *J Atmos Sol Terr Phys*, 63(18):1891–1900.

Mendoza, B., Velasco, V., and J´auregui, E. (2006). A study of historical droughts in southeastern Mexico. *J Clim*, 19(12):2916–2934.

Mo, K. C., Schemm, J.-K. E., and Yoo, S.-H. (2009). Influence of ENSO and the Atlantic Multidecadal Oscillation on drought over the United States. *J Clim*, 22(22):5962–5982.

Moazami, A., Nik, V. M., Carlucci, S., and Geving, S. (2019). Impacts of future weather data typology on building energy performance–Investigating long-term patterns of climate change and extreme weather conditions. *App Energy*, 238:696–720.

Moy, C. M., Seltzer, G. O., Rodbell, D. T., and Anderson, D. M. (2002). Variability of El Niño/Southern Oscillation activity at millennial timescales during the Holocene epoch. *Nature*, 420(6912):162.

Nalley, D., Adamowski, J., Khalil, B., and Ozga-Zielinski, B. (2013). Trend detection in surface air temperature in Ontario and Quebec, Canada during 1967–2006 using the discrete wavelet transform. *Atmos Res*, 132:375–398.

Nastos, P. and Zerefos, C. (2007). On extreme daily precipitation totals at Athens, Greece. *Adv Geosci*, 10:59–66.

National Center for Atmospheric Research Staff (Eds). (2013). *The Climate Data Guide: QBO: Quasi-Biennial Oscillation.* Retrieved from https://climatedataguide.ucar.edu/climate-data/qbo-quasi-biennial-oscillation

National Center for Atmospheric Research Staff (Eds). (2020). *The Climate Data Guide: Hurrell wintertime SLP-based Northern Annular Mode (NAM) Index.* Retrieved from https://climatedataguide.ucar.edu/climate-data/hurrell-wintertime-slp-based-northern-annular-mode-nam-index

Nye, J. A., Link, J. S., Hare, J. A., and Overholtz, W. J. (2009). Changing spatial distribution of fish stocks in relation to climate and population size on the Northeast United States continental shelf. *Mar Ecol Prog Ser*, 393:111–129.

Oliver, E. C., Burrows, M. T., Donat, M. G., Sen Gupta, A., Alexander, L. V., Perkins-Kirkpatrick, S. E., Benthuysen, J., Hobday, A. J., Holbrook, N. J., Moore, P. J. and Thomsen, M. S. (2019). Projected marine heatwaves in the 21st century and the potential for ecological impact. *Front Mar Sci*, *6*, 734.

Olsen, J., Anderson, N. J., and Knudsen, M. F. (2012). Variability of the North Atlantic Oscillation over the past 5,200 years. *Nature Geosci*, 5(11):808–812.

Panda, D. K., Panigrahi, P., Mohanty, S., Mohanty, R. K., and Sethi, R. R. (2016). The 20th century transitions in basic and extreme monsoon rainfall indices in India: Comparison of the ETCCDI indices. *Atmos Res*, *181*, 220-235.

Park, J.-H. and Li, T. (2019). Interdecadal modulation of El Niño–tropical North Atlantic teleconnection by the Atlantic Multi-decadal Oscillation. *Clim Dyn*, 52(9-10):5345–5360.

Patterson, R. T. and Swindles, G. T. (2015). Influence of ocean–atmospheric oscillations on lake ice phenology in eastern North America. *Clim Dyn*, 45(910):2293–2308.

Payette, S., Filion, L., Gauthier, L., and Boutin, Y. (1985). Secular climate change in old-growth tree-line vegetation of northern Quebec. *Nature*, 315(6015):135–138.

Perkins-Kirkpatrick, S. and Lewis, S. (2020). Increasing trends in regional heatwaves. *Nature Commun*, 11(1):1–8.

Perkins-Kirkpatrick, S. E., Fischer, E. M., Ang´elil, O., and Gibson, P. B. (2017). The influence of internal climate variability on heatwave frequency trends. *Environ Res Lett*, 12(4):044005.

Prokoph, A., Patterson, R.T. (2004). Application of wavelet and regression analysis in assessing temporal and geographic climate variability: Eastern Ontario, Canada as a case study. *Atmos Ocean*, 42 (3):201-212.

Prokoph, A., Adamowski, J. and Adamowski, K., (2012). Influence of the 11 year solar cycle on annual streamflow maxima in Southern Canada. *J Hydrol*, *442*:55-62.

Quiroz, R. S. (1981). Period modulation of the stratospheric Quasi-Biennial Oscillation. *Mon Weather Rev*, 109(3):665–674.

Rahmstorf, S. and Coumou, D. (2011). Increase of extreme events in a warming world. *Proc Natl Acad Sci*, 108(44):17905–17909.

Rigor, I. G., Wallace, J. M., and Colony, R. L. (2002). Response of sea ice to the Arctic Oscillation. *J Clim*, 15(18):2648–2663.

Rind, D., Lean, J., Lerner, J., Lonergan, P., and Leboissitier, A. (2008). Exploring the stratospheric/tropospheric response to solar forcing. *J Geophys Res: Atmos*, 113(D24).

Rodbell, D. T., Seltzer, G. O., Anderson, D. M., Abbott, M. B., Enfield, D. B., and Newman, J. H. (1999). An ~15,000-year record of El Niño-driven alluviation in southwestern Ecuador. *Science*, 283(5401):516–520.

Ropelewski, C. F. and Halpert, M. S. (1986). North American precipitation and temperature patterns associated with the El Niño/Southern Oscillation (ENSO). *Mon Weather Rev*, 114(12):2352–2362.

Ruiz-Barradas, A., Nigam, S. and Kavvada, A., (2013). The Atlantic Multidecadal Oscillation in twentieth century climate simulations: uneven progress from CMIP3 to CMIP5. *Clim Dyn*, *41*(11-12):3301-3315.

Schlesinger, M. E. and Ramankutty, N. (1994). An oscillation in the global climate system of period 65–70 years. *Nature*, 367(6465):723–726.

Schulz, M. and Mudelsee, M. (2002). REDFIT: estimating red-noise spectra directly from unevenly spaced paleoclimatic time series. *Comput Geosci*, 28(3):421–426.

Scott, D., McBoyle, G., and Mills, B. (2003). Climate change and the skiing industry in southern Ontario (Canada): exploring the importance of snowmaking as a technical adaptation. *Clim Research*, 23(2):171–181.

Seo, J., Choi, W., Youn, D., Park, D.-S. R., and Kim, J. Y. (2013). Relationship between the stratospheric Quasi-Biennial Oscillation and the spring rainfall in the western North Pacific. *Geophys Res Lett*, 40(22):5949–5953.

Sfîcă, L., Iordache, I., and Voiculescu, M. (2018). Solar signal on regional scale: a study of possible solar impact upon Romania's climate. *J Atmos Sol Terr Phys*, 177:257–265.

Sharma, S. and Magnuson, J. J. (2014). Oscillatory dynamics do not mask linear trends in the timing of ice breakup for Northern Hemisphere lakes from 1855 to 2004. *Clim Change*, 124(4):835–847.

Steinschneider, S. and Brown, C. (2011). Influences of North Atlantic climate variability on low-flows in the Connecticut River Basin. *J Hydrol*, 409(1-2):212–224.

Stephenson, D. B., Diaz, H., and Murnane, R. (2008). Definition, diagnosis, and origin of extreme weather and climate events. *Clim Extrem Soc*, 340:11–23.

Stockwell, J.D., Doubek, J.P., Adrian, R., Anneville, O., Carey, C.C., Carvalho, L., De Senerpont Domis, L.N., Dur, G., Frassl, M.A., Grossart, H.P. and Ibelings, B.W. (2020). Storm impacts on phytoplankton community dynamics in lakes. *Glob Change Biol*, 26(5):2756-2784.

Sunspot Index and Long Term Solar Observations (SILSO). (2021). Total sunspot number. Royal Observatory of Belgium, Brussels, Belgium. Retrieved from http://www.sidc.be/silso/datafiles

Sutton, R. T. and Hodson, D. L. (2005). Atlantic Ocean forcing of North American and European summer climate. *Science*, 309(5731):115–118.

Sutton, R. T. and Hodson, D. L. (2007). Climate response to basin-scale warming and cooling of the North Atlantic Ocean. *J Clim*, 20(5):891–907.

Tan, X. and Gan, T. Y. (2017). Non-stationary analysis of the frequency and intensity of heavy precipitation over Canada and their relations to large-scale climate patterns. *Clim Dyn*, 48(9-10):2983-3001.

Thomson, D. J. (1982). Spectrum estimation and harmonic analysis. *Proc IEEE*, 70(9):1055–1096.

Thresher, R. E. (2002). Solar correlates of Southern Hemisphere mid-latitude climate variability. *Int J Clim*, 22(8):901–915.

Trewartha, G. and Horn, L. (1980). Koppen's classification of climates. *An Introduction to climate. McGraw-Hill, New York*, pages 397–403.

Trenberth, K. and National Center for Atmospheric Research Staff (Eds). (2020). *The Climate Data Guide: Nino SST Indices (Nino 1+2, 3, 3.4, 4; ONI and TNI*). Retrieved from https://climatedataguide.ucar.edu/climate-data/nino-sst-indices-nino-12-3-34-4-oni-and-tni

Trenberth, K., Zhang, R., and National Center for Atmospheric Research Staff (Eds). (2021). *The Climate Data Guide: Atlantic Multi-decadal Oscillation (AMO).* Retrieved from https://climatedataguide.ucar.edu/climate-data/atlantic-multi-decadal-oscillation-amo

Ugarte, R. A., Craigie, J. S., and Critchley, A. T. (2010). Fucoid flora of the rocky intertidal of the Canadian Maritimes: implications for the future with rapid climate change. In *Seaweeds and their role in globally changing environments*, pages 69–90. Springer.

van Loon, H., Meehl, G. A., and Arblaster, J. M. (2004). A decadal solar effect in the tropics in July–August. *J Atmos Sol Terr Phys*, 66(18):1767–1778.

van Loon, H. and Shea, D. J. (1999). A probable signal of the 11-year solar cycle in the troposphere of the Northern Hemisphere. *Geophys Res Lett*, 26(18):2893–2896.

Vincent, L., Zhang, X., Mekis, E., Wan, H., and Bush, E. (2018). Changes in Canada's climate: Trends in indices based on daily temperature and precipitation data. *Atmos Ocean*, 56(5):332-349.

Vines, R. (1977). Possible relationships between rainfall, crop yields and the Sunspot cycle. *J Aust Inst Agric Sci*, 43(1-2):3–13.

Vines, R. (1980). Analyses of South African rainfall. *South Afr J Sci*, 76(9):404–409.

Vines, R. (1984). Rainfall patterns in the eastern United States. *Clim Change*, 6(1):79– 98.

Vines, R. (1986). Rainfall patterns in India. *J Climatol*, 6(2):135–148.

Wang, X., Thompson, D. K., Marshall, G. A., Tymstra, C., Carr, R., and Flannigan, M. D. (2015). Increasing frequency of extreme fire weather in Canada with climate change. *Clim Change*, 130(4):573–586.

Waple, A., Mann, M., and Bradley, R. (2002). Long-term patterns of solar irradiance forcing in model experiments and proxy based surface temperature reconstructions. *Clim Dyn*, 18(7):563–578.

Ward Jr, J. H. (1963). Hierarchical grouping to optimize an objective function. *J Am Statistical Assoc*, 58(301):236–244.

Wolter, K., Dole, R. M., and Smith, C. A. (1999). Short-term climate extremes over the continental United States and ENSO. Part I: Seasonal temperatures. *J Clim*, 12(11):3255–3272.

World Economic Forum. (2019). The global risks report (14th ed.). Geneva, Switzerland: World Economic Forum.

Yang, Y., Gan, T. Y., and Tan, X. (2020). Spatiotemporal changes of drought characteristics and their dynamic drivers in Canada. *Atmos Res*, 232:104695.

Young, G. H., McCarroll, D., Loader, N. J., Gagen, M. H., Kirchhefer, A. J., and Demmler, J. C. (2012). Changes in atmospheric circulation and the Arctic Oscillation preserved within a millennial length reconstruction of summer cloud cover from northern Fennoscandia. *Clim Dyn*, 39(1-2):495–507.

Zar, Jerrold H. (1998). Biostatistical Analysis (4th ed.). Upper Saddle River, N.J.: Prentice Hall. pp. 43–45.

Zhang, L., Wang, C., and Wu, L. (2012). Low-frequency modulation of the Atlantic warm pool by the Atlantic Multidecadal Oscillation. *Clim Dyn*, 39(78):1661–1671.

Zhang, W., Mei, X., Geng, X., Turner, A. G., and Jin, F.-F. (2019). A nonstationary ENSO–NAO relationship due to AMO modulation. *J Clim*, 32(1):33–43.

Zhang, X., Hogg, W., and Mekis, E. (2001). Spatial and temporal characteristics of heavy precipitation events over Canada. *J Clim*, 14(9):1923-1936.

Zhou, Q., Chen, W., and Zhou, W. (2013). Solar cycle modulation of the ENSO impact on the winter climate of East Asia. *J Geophys Res: Atmos*, 118(11):5111–5119.

Ziska, L. H., Epstein, P. R., and Rogers, C. A. (2008). Climate change, aerobiology, and public health in the Northeast United States. *Mitig Adapt Strategies Glob Change*, 13(5-6):607–613.

Figures

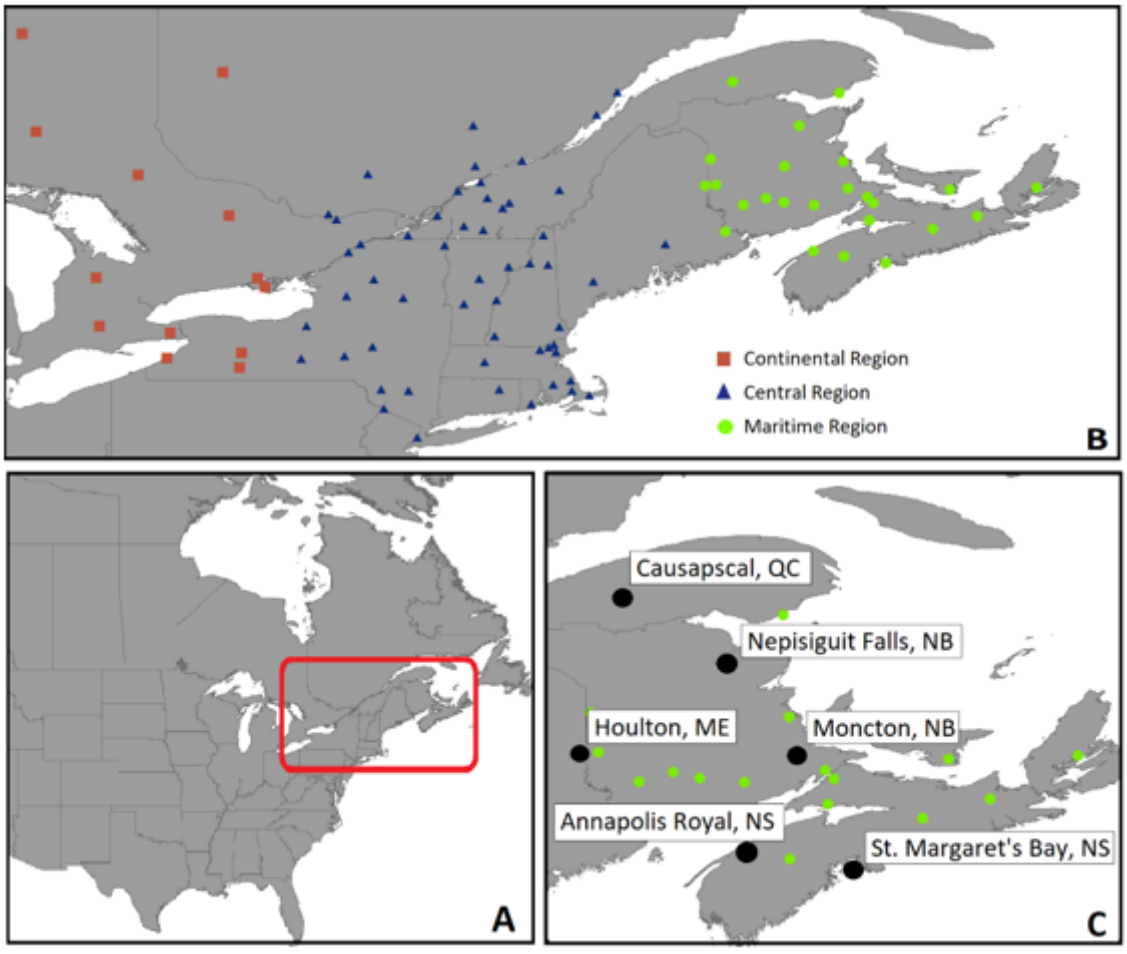

Figure 1

A) Map showing area of eastern North America covered in this research B) locations of weather stations with high quality long–term weather records, and subdivided into three smaller climatic regions (Continental Region, Central Region, Maritime Region) using cluster analysis, C) Close-up of the Maritime Region climate zone showing locations of climate stations with high quality climatic records, with six exemplary stations analyzed in detail here highlighted in black

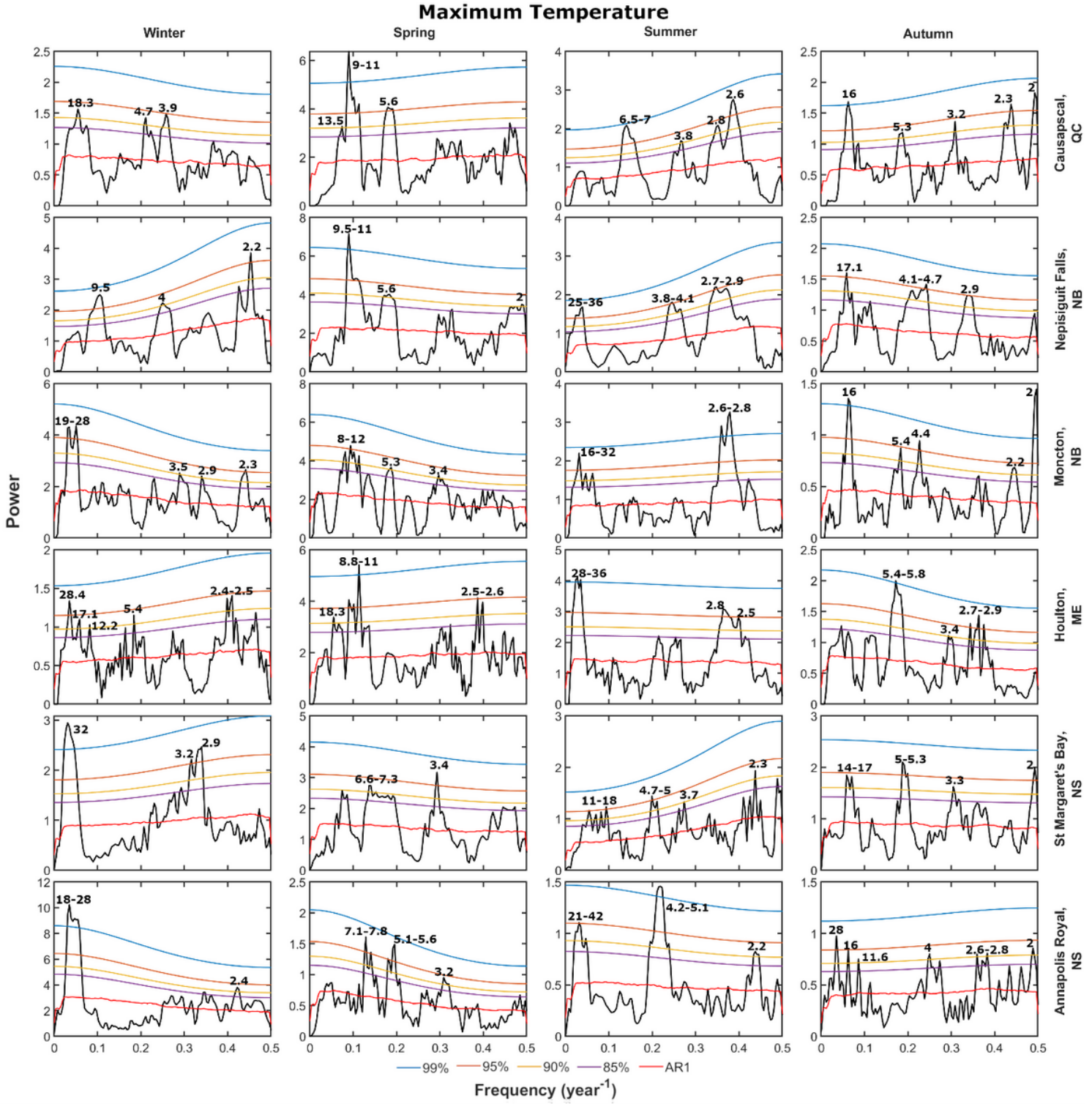

Figure 2

Red noise spectral analysis for extreme maximum temperature records at the six stations used in this study, with AR1 and various confidence levels indicated. All peaks above 90% confidence are labelled in years

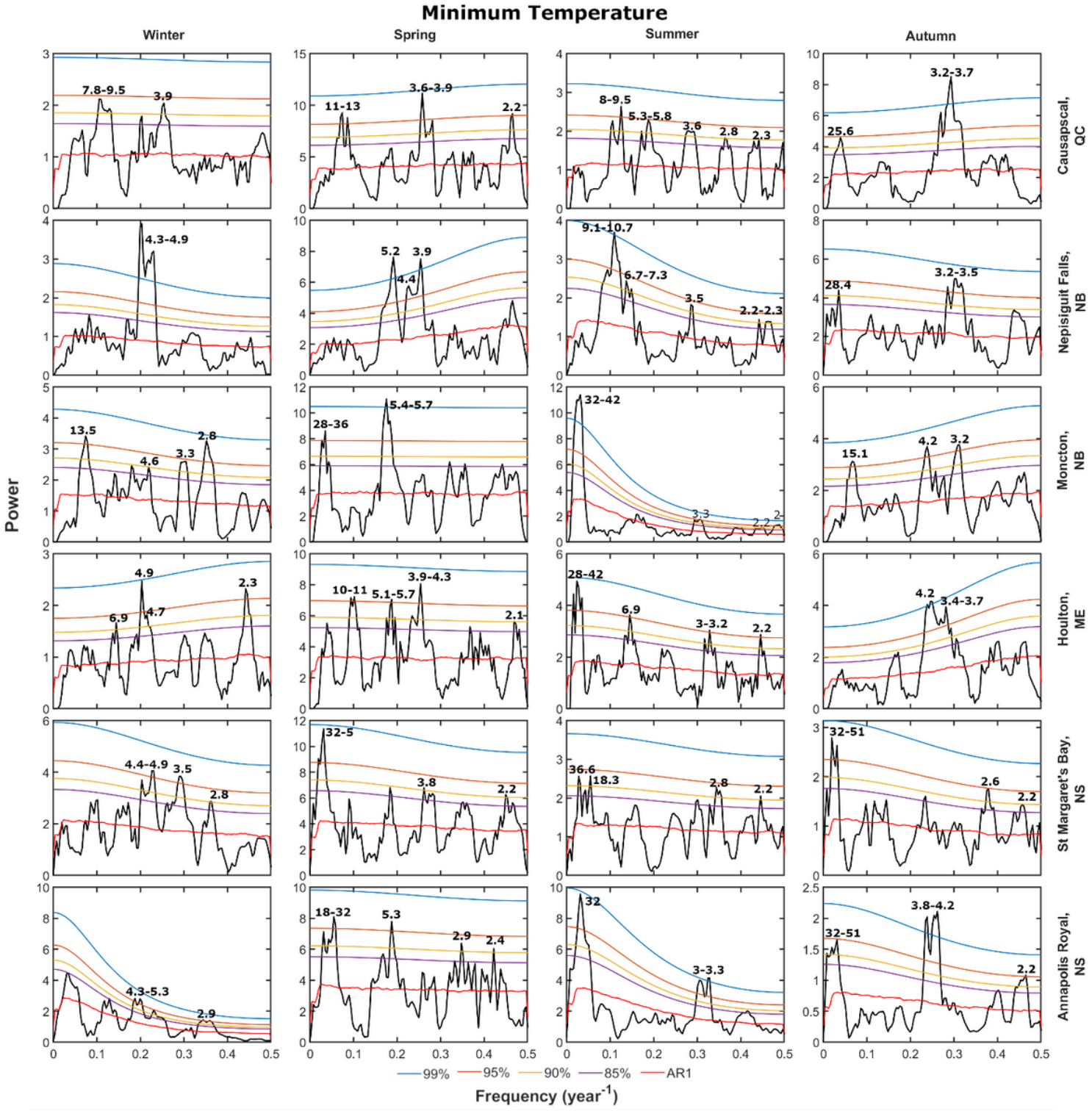

Figure 3

Red noise spectral analysis for extreme minimum temperature records at the six stations used in this study, with AR1 and various confidence levels indicated. All peaks above 90% confidence are labelled in

years

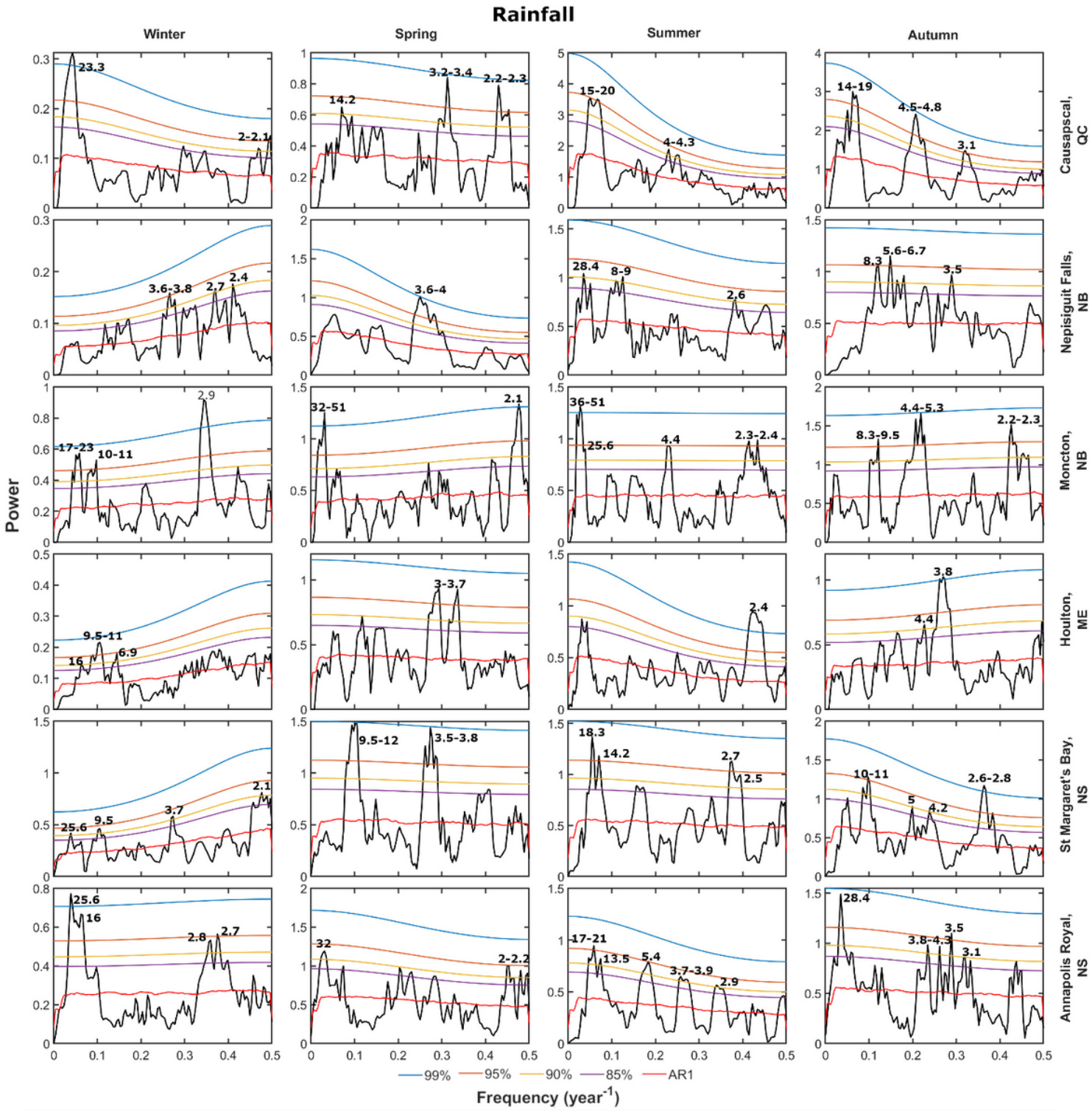

Figure 4

Red noise spectral analysis for extreme rainfall records at the six stations used in this study, with AR1 and various confidence levels indicated. All peaks above 90% confidence are labelled in years

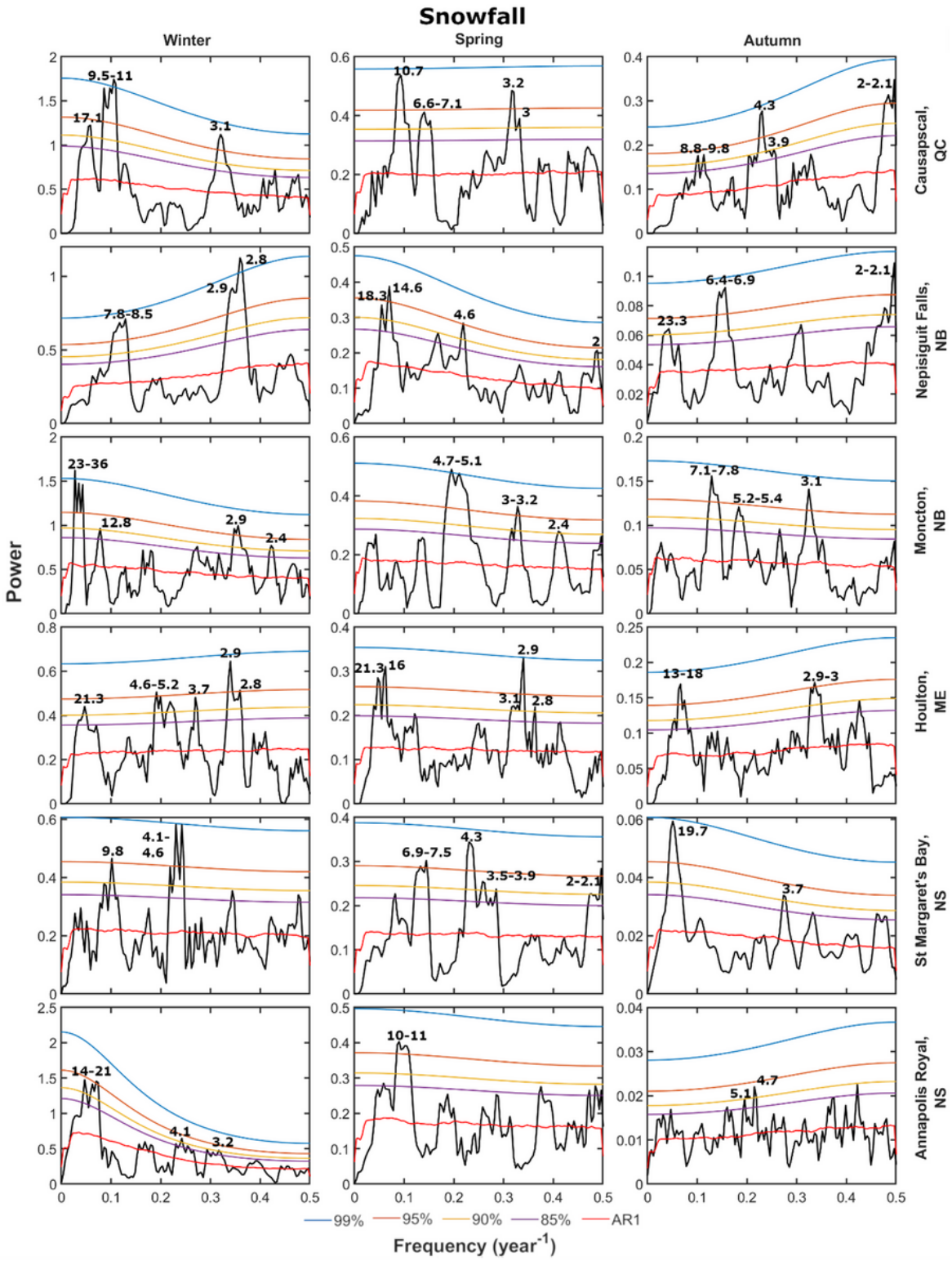

Figure 5

Red noise spectral analysis for extreme snowfall at the six stations used in this study, with AR1 and various confidence levels indicated. All peaks above 90% confidence are labelled in years

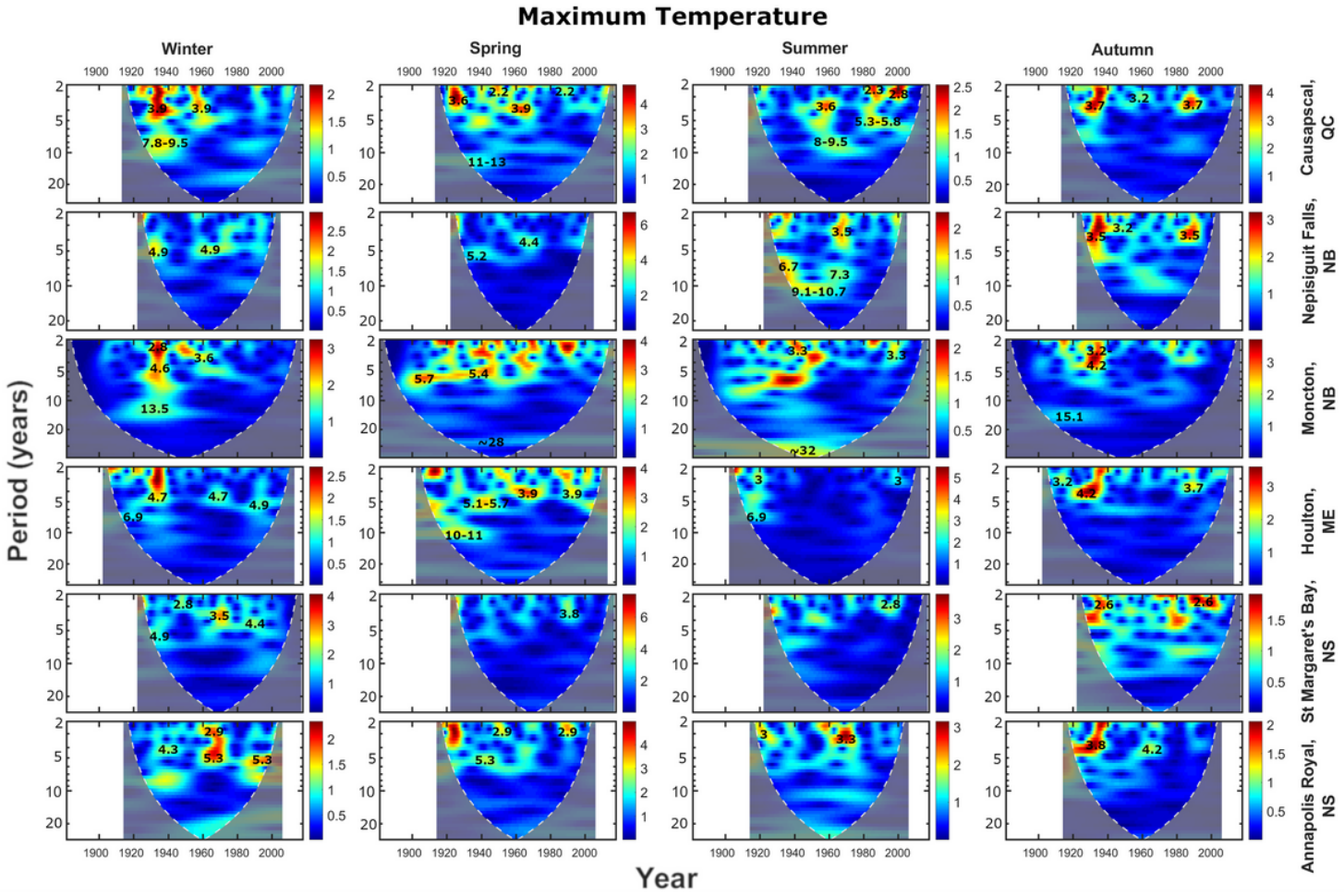

Figure 6

Continuous wavelet transforms (CWTs) for extreme maximum temperature records at the six stations used in this study Areas of high spectral density that are greater than the 90% confidence level are labelled with the cycle length in years

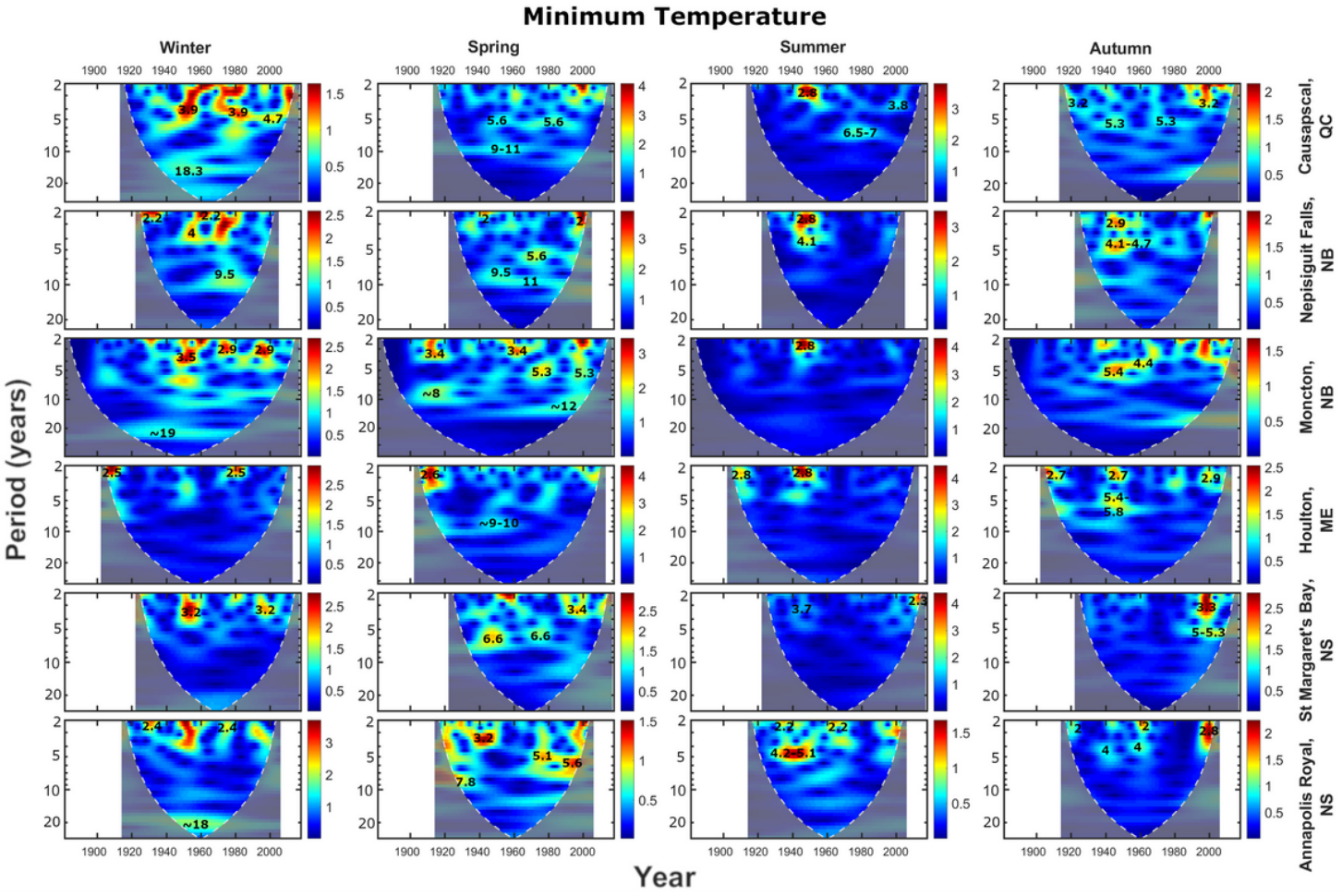

Figure 7

Continuous wavelet transforms (CWTs) for extreme minimum temperature records at the six stations used in this study. Areas of high spectral density that are greater than the 90% confidence level are labelled with the cycle length in years

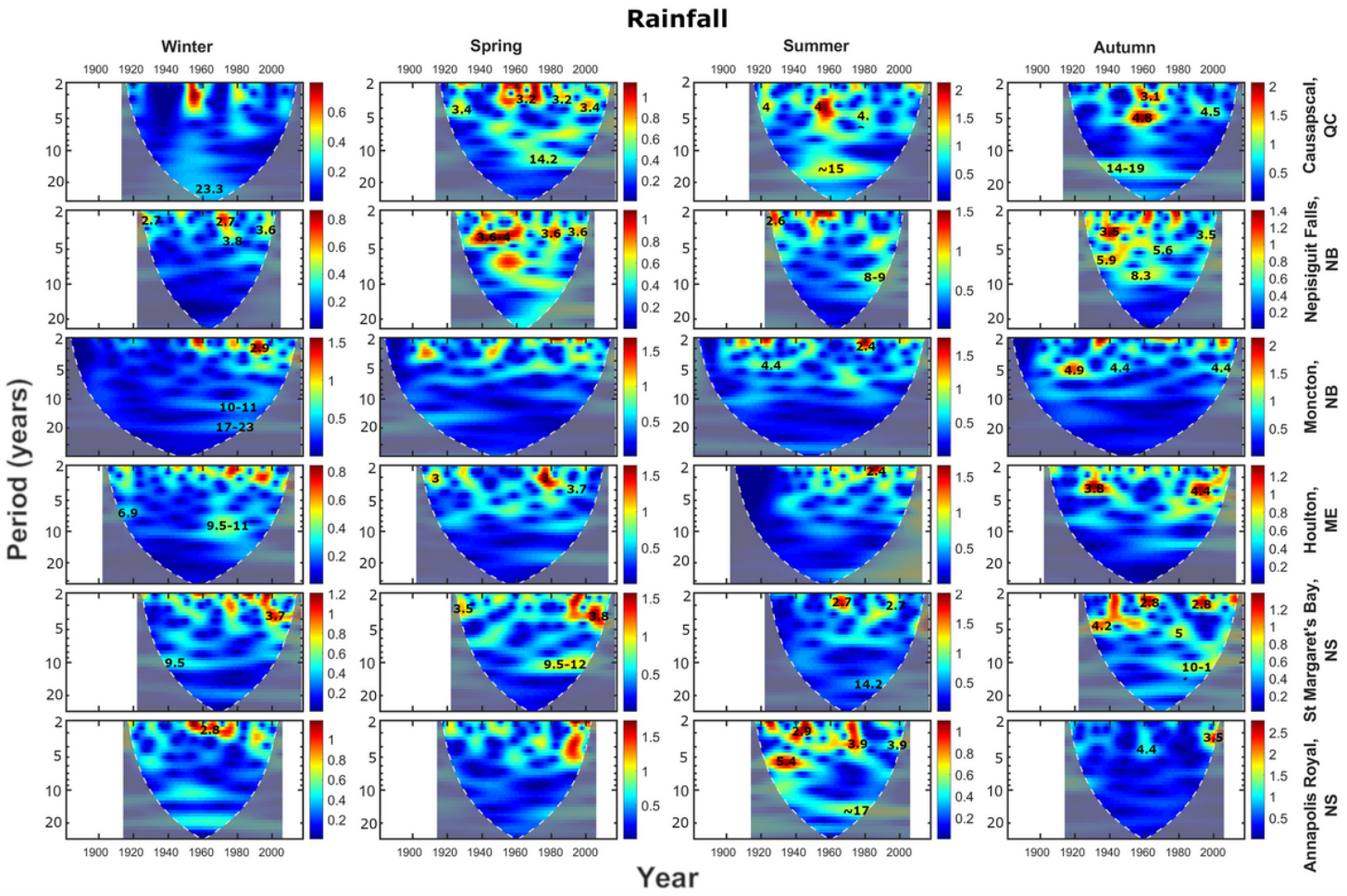

Figure 8

Continuous wavelet transforms (CWTs) for extreme rainfall records at the six stations used in this study. Areas of high spectral density that are greater than the 90% confidence level are labelled with the cycle length in years

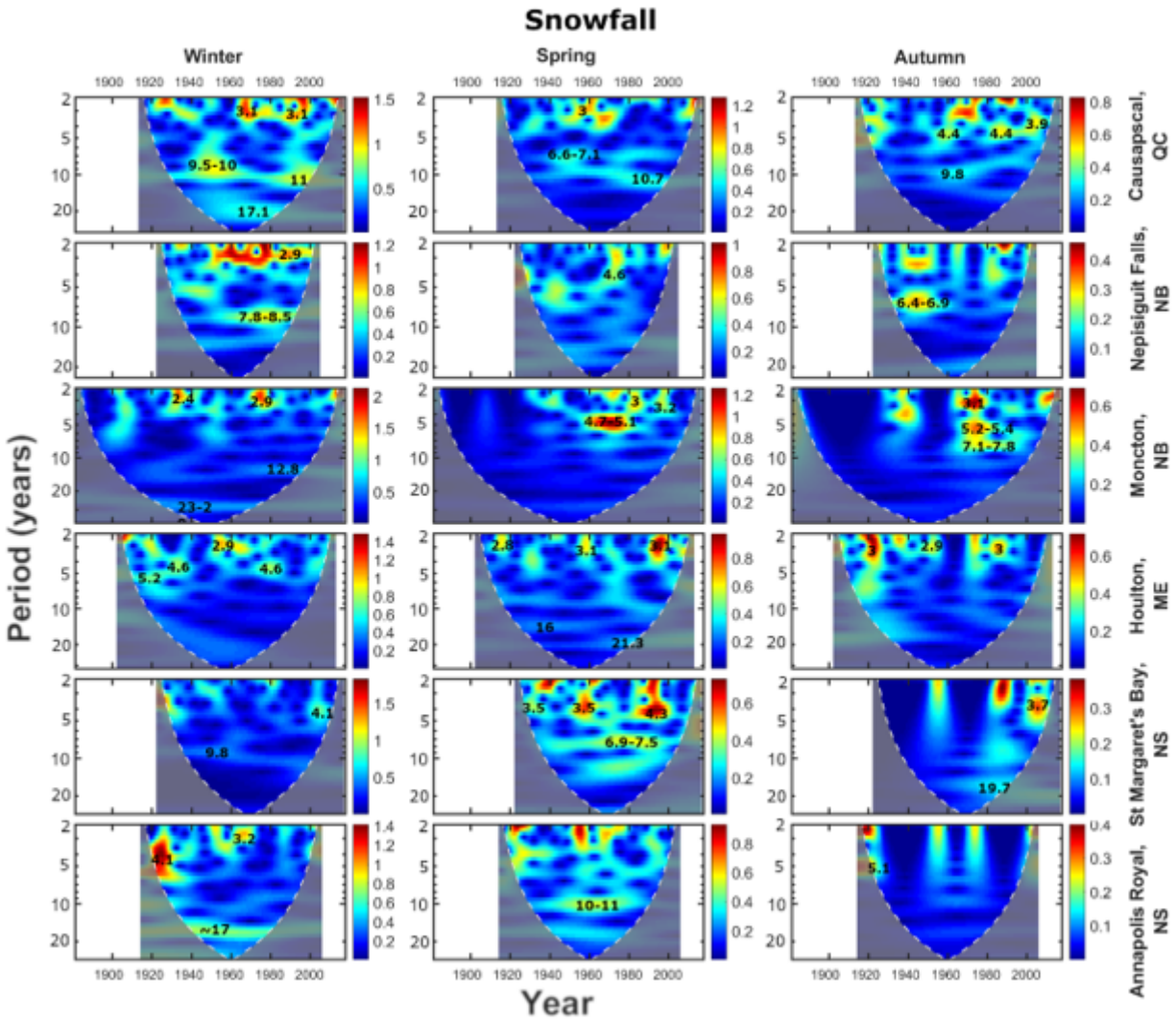

Figure 9

Continuous wavelet transforms (CWTs) for extreme snowfall records at the six stations used in this study. Areas of high spectral density that are greater than the 90% confidence level are labelled with the cycle length in years

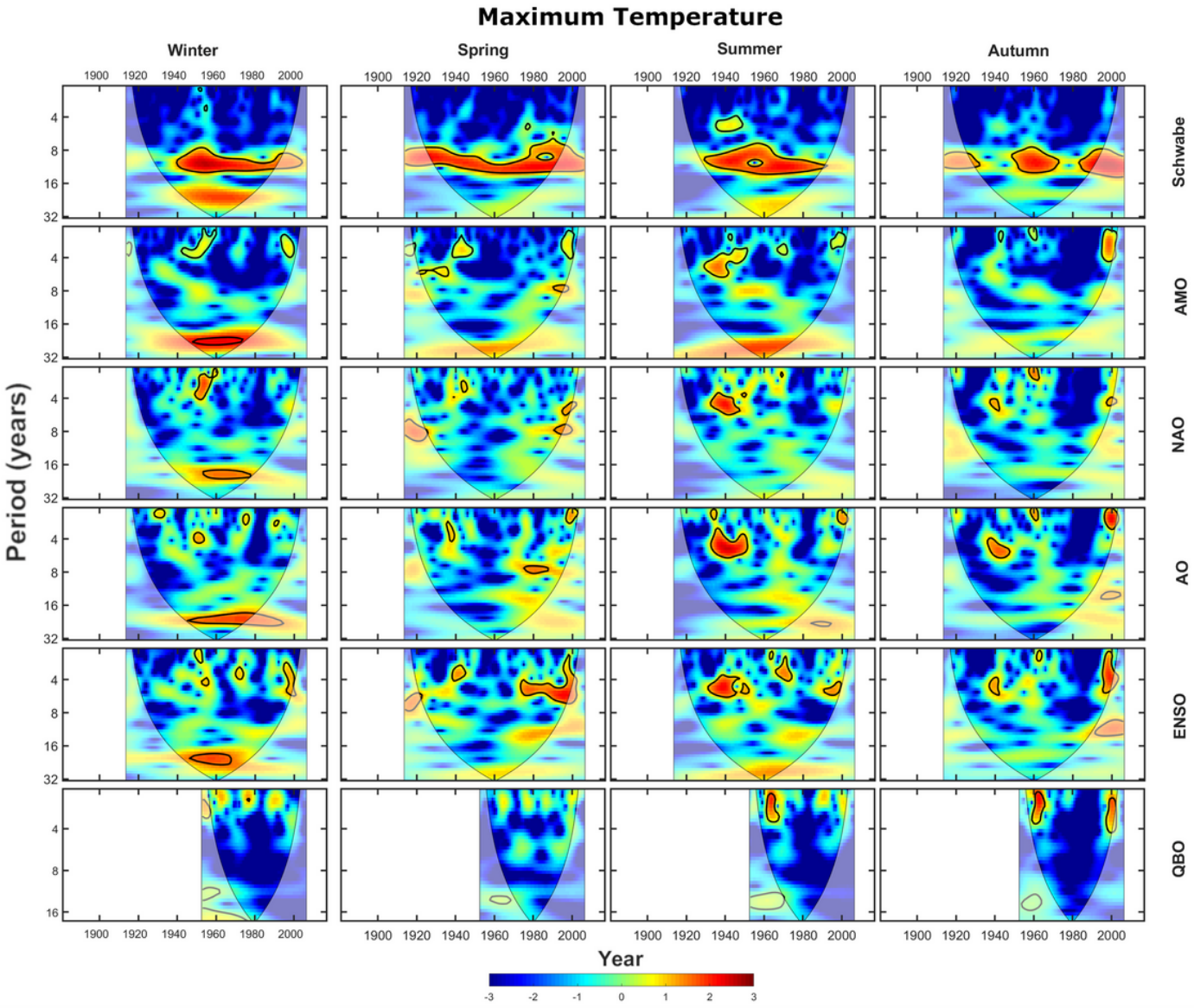

Figure 10

Cross wavelet transforms (XWT) of the extreme maximum temperature record for Annapolis Royal, NS and various climate oscillations

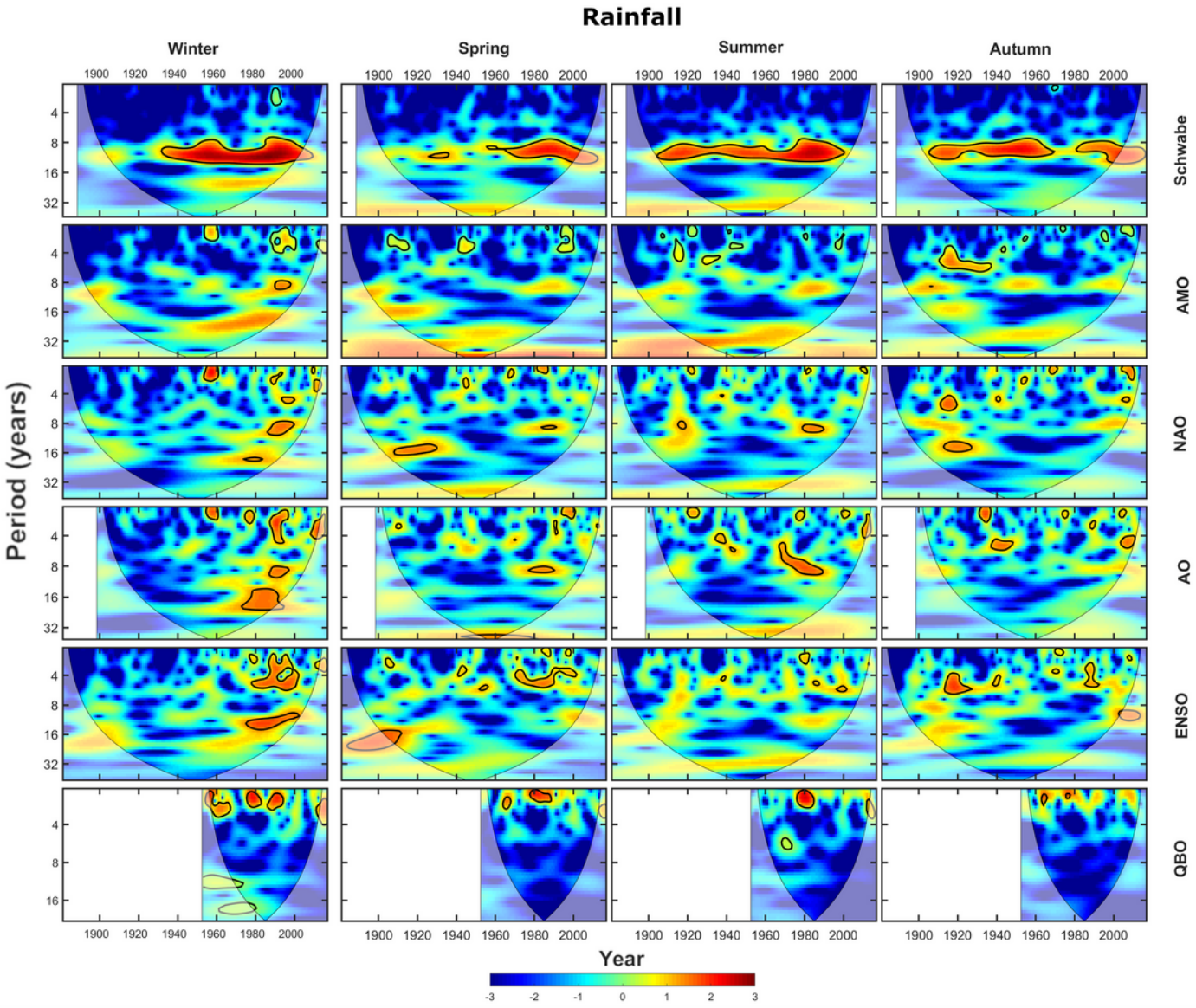

Figure 11

Cross wavelet transforms (XWT) of the extreme rainfall record for Moncton, NB and various climate oscillations

Supplementary Files

This is a list of supplementary files associated with this preprint. Click to download.

- SupplementaryMaterial.docx